(12) INTERNATIONAL APPLICATION PUBLISHED UNDER THE PATENT COOPERATION TREATY (PCT)

(19) World Intellectual Property Organization
International Bureau

(43) International Publication Date
13 February 2025 (13.02.2025)

WIPO | PCT

(10) International Publication Number
WO 2025/032550 A1

(51) International Patent Classification:
A61K 31/04 (2006.01) *A61P 25/00* (2006.01)
C12Q 1/68 (2018.01) *A61P 25/28* (2006.01)
A61P 25/18 (2006.01) *C12Q 1/686* (2018.01)

(21) International Application Number:
PCT/IB2024/057742

(22) International Filing Date:
09 August 2024 (09.08.2024)

(25) Filing Language: English

(26) Publication Language: English

(30) Priority Data:
63/531,913 10 August 2023 (10.08.2023) US

(71) Applicant: **RAMOT AT TEL-AVIV UNIVERSITY LTD.** [IL/IL]; P.O. Box 39296, 6139201 Tel Aviv (IL).

(72) Inventors: **SHOMRON, Noam**; c/o Ramot at Tel-Aviv University Ltd., P.O. Box 39296, 6139201 Tel Aviv (IL). **ISRAEL-ELGALI, Ifat**; c/o Ramot at Tel-Aviv University Ltd., P.O. Box 39296, 6139201 Tel Aviv (IL). **GURWITZ, David**; c/o Ramot at Tel-Aviv University Ltd., P.O. Box 39296, 6139201 Tel Aviv (IL).

(74) Agent: **FISHER, Zeev**; 32B Habarzel Street, 6971048 Tel Aviv (IL).

(81) Designated States *(unless otherwise indicated, for every kind of national protection available)*: AE, AG, AL, AM, AO, AT, AU, AZ, BA, BB, BG, BH, BN, BR, BW, BY, BZ, CA, CH, CL, CN, CO, CR, CU, CV, CZ, DE, DJ, DK, DM, DO, DZ, EC, EE, EG, ES, FI, GB, GD, GE, GH, GM, GT, HN, HR, HU, ID, IL, IN, IQ, IR, IS, IT, JM, JO, JP, KE, KG, KH, KN, KP, KR, KW, KZ, LA, LC, LK, LR, LS, LU, LY, MA, MD, MG, MK, MN, MU, MW, MX, MY, MZ, NA, NG, NI, NO, NZ, OM, PA, PE, PG, PH, PL, PT, QA, RO, RS, RU, RW, SA, SC, SD, SE, SG, SK, SL, ST, SV, SY, TH, TJ, TM, TN, TR, TT, TZ, UA, UG, US, UZ, VC, VN, WS, ZA, ZM, ZW.

(84) Designated States *(unless otherwise indicated, for every kind of regional protection available)*: ARIPO (BW, CV, GH, GM, KE, LR, LS, MW, MZ, NA, RW, SC, SD, SL, ST, SZ, TZ, UG, ZM, ZW), Eurasian (AM, AZ, BY, KG, KZ, RU, TJ, TM), European (AL, AT, BE, BG, CH, CY, CZ, DE, DK, EE, ES, FI, FR, GB, GR, HR, HU, IE, IS, IT, LT, LU, LV, MC, ME, MK, MT, NL, NO, PL, PT, RO, RS, SE, SI, SK, SM, TR), OAPI (BF, BJ, CF, CG, CI, CM, GA, GN, GQ, GW, KM, ML, MR, NE, SN, TD, TG).

Published:
— *with international search report (Art. 21(3))*
— *in black and white; the international application as filed contained color or greyscale and is available for download from PATENTSCOPE*

(54) Title: COMPOSITION AND METHOD FOR THE TREATMENT OF MYELIN STRUCTURAL DEFICIENCIES

(57) Abstract: Methods and compositions are disclosed for treating myelin structural deficiencies and restoring normal myelin structure. This is achieved by downregulating Qki to increase Myelin Basic Protein (MBP) production, using selective serotonin reuptake inhibitors (SSRIs) such as citalopram to enhance expression of miR-30b-5p and miR-101a-3p. miRNA mimics can also be employed to achieve similar outcomes. The methods include administering SSRIs, miRNA mimics, utilizing Adeno-Associated Virus (AAV) vectors for gene delivery, or using intranasal delivery systems for encapsulated miRNAs. These approaches are applicable to a range of conditions, including Major Depressive Disorder (MDD), schizophrenia, bipolar disorder, and other CNS disorders. Methods for developing therapeutic agents, assessing treatment efficacy, and detecting said conditions using biomarkers of miR-30b-5p, miR-101a-3p, and Qki are also disclosed.

WO 2025/032550 A1

COMPOSITION AND METHOD FOR THE TREATMENT OF MYELIN STRUCTURAL DEFICIENCIES

FIELD OF THE INVENTION

[0001] The present disclosure relates to compositions and methods for the treatment of myelin structural deficiencies to restore normal myelin structure as well as compositions and methods for treating various conditions related to myelin deficiencies. Specifically, the compositions and treatments involve increasing expression levels of miR-30b-5p and miR-101-3p resulting in downregulation of their target gene, Qki, and an increase of myelin basic protein (MBP) production resulting in restoration of myelin structure and mitigation of conditions and symptoms related to myelin structural deficiencies.

BACKGROUND

[0001] The Raphe Nuclei (RN) are a group of nuclei located in the brainstem that consists of serotonergic synthesizing neurons which assemble the major ascending serotonergic fibers projecting to the forebrain and descending fibers that extend to the medulla and spinal cord. Through its ascending projections, the RN has an important role in the regulation of many physiological functions, including learning, cognition, and mood.

[0002] Myelin is a lipid-rich electrically insulating tissue crucial for electrical communication and transmission of axon potentials between neurons and provides metabolic support to the axons it ensheaths. Oligodendrocytes are the myelinating cells of the CNS. They are generated from oligodendrocyte progenitor cells and are essential for myelin formation and regeneration, for example, in multiple sclerosis. MBP is a main protein in myelin and is expressed on the cytoplasmic surface of the oligodendrocyte plasma membrane. Oligodendrocytes express serotonin receptors and were shown to be affected by serotonin, 5-HT receptor agonists and SSRI administration.

[0003] Myelination related deficits, oligodendrocyte morphometry changes, and white matter abnormalities were previously shown to be involved in various psychiatric disorders such as schizophrenia, alcoholism, bipolar disorder and Major Depressive Disorder (MDD). Myelination deficits have also been observed in several additional CNS disorders (or their mouse models), such as Alzheimer's disease, Parkinson's disease, Autism, Anorexia, and PTSD. Most importantly, the prevalence of MDD and anxiety disorders among individuals with multiple sclerosis, a demyelinating disease of the CNS, highlights the connection between myelin deficits and MDD symptoms. Certain studies showed no change in oligodendrocyte density in MDD, suggesting unchanged morphology despite possible organizational disruption. The disruption might result from altered myelin-related gene expression or splicing; and consequently, present in myelin related proteins, or as abnormalities in transcription factors of myelin-related genes. Thus, the association of myelin deficits in the RN underscores the importance of addressing myelin integrity in therapeutic strategies aimed at treating or mitigating these disorders.

[0004] MicroRNAs are single-stranded, short endogenous non-coding RNAs present in all cells and tissues that down-regulate gene expression at the post-transcriptional level. Thousands of miRNAs are encoded within the human or rodent genome, and their dysregulation has been implicated in many chronic diseases, including brain disorders. As changes in miRNA levels affect global gene expression, miRNAs have been proposed as biomarkers for disease diagnosis and treatment choice, including for CNS disorders. miRNAs have been related to neuro-inflammation, altered neurogenesis, neuroplasticity, stress response and circadian rhythms, and factors implicated in MDD pathogenesis; all of which may be affected by antidepressant treatment. Thus, study of miRNAs alongside antidepressant treatment can provide insight into other potential treatments for MDD and other neurological and neuropsychiatric disorders.

[0005] MDD is a complex, common, and recurrent mental disorder and is among the leading global causes of disability, affecting more than 250 million people annually,

and is more commonly diagnosed in women than in men. The monoamine hypothesis of depression, formulated over 40 years ago, proposes the biological basis of depression results from a central nervous system (CNS) imbalance or decrease in the neurotransmitter serotonin (5-HT). This decrease might be due to increased serotonin transporter (SERT) activity, reduced serotonin synthesis in the CNS or damage to CNS serotonergic synapses following chronic stress conditions. Thus, the current first-line treatment for MDD is selective serotonin reuptake inhibitors (SSRIs), which are antidepressant drugs that block serotonin reuptake by binding to SERT.

[0006] The longstanding monoamine hypothesis suggests that SSRIs relieve depression symptoms mainly via blocking SERT, thereby increasing the availability of serotonin in serotonergic CNS synapses. However, while SERT inhibition is achieved within a few days of initiating SSRI treatment, remission from depression starts after about 4 weeks. This discrepancy in time led to the suggestion that recovery from depression involves synaptogenesis and neurogenesis. However, it is unclear whether SSRI-mediated SERT blockage is involved in these two processes.

[0007] The present disclosure explores the interrelationships between the effects of the SSRI citalopram on relief from depression-like symptoms, RN myelin integrity, and RN microRNA expression in the chronic unpredictable stress (CUS) mouse model for depression. The disclosure shows that chronic stress causes depressive-like symptoms and RN defects in myelin structure, and these symptoms can be prevented by daily citalopram administration, which was correlated with increased expression levels of miR-30b-5p and miR-101-3p. Accordingly, elevated Qki expression levels were observed in the RN of CUS mice, which affected Mbp expression and myelin structure – all of which were prevented by citalopram administration as it resulted in increased expression levels of miR-30b-5p and miR-101-3p. The present disclosure suggests that SSRI's such as citalopram, as well as miRNAs such as miR-30b-5p and miR-101-3p, can restore normal myelin structure by downregulating Qki and allowing for increased expression of Mbp. This has important implications regarding the treatment of a wide variety of conditions involving myelin deficiencies, including MDD.

[0008] Therefore, the present disclosure relates to compositions and methods for treating conditions related to myelin deficiencies by promoting elevated expression levels of miR-30b-5p and miR-101-3p such as through administration of SSRI's such as citalopram and through other compositions and methods described herein.

SUMMARY OF THE INVENTION

[0009] The present disclosure investigates treatment of MDD which provides cross-indicational data for evaluating potential therapeutic strategies for a variety of other conditions caused by myelin deficiencies. By focusing on MDD, which shares common pathophysiological mechanisms with conditions such as schizophrenia, bipolar disorder, Parkinson's disease, and Alzheimer's disease, this disclosure informs treatments for these related disorders as well. The results of the present disclosure establish the broader applicability of the presently disclosed therapeutic interventions which target myelin deficiencies and can be used to treat a variety of neurological and neuropsychiatric conditions.

[0010] MDD is the most common and widespread mental disorder. Selective serotonin reuptake inhibitors (SSRIs) are the first-line treatment for MDD. The relation between the inhibition of serotonin reuptake in the central nervous system and remission from MDD remains controversial, as reuptake inhibition occurs rapidly, but remission from MDD takes weeks to months. Myelination-related deficits and white matter abnormalities were shown to be involved in psychiatric disorders such as MDD and a variety of others. This can explain the delay in remission following SSRI administration. The RN, located in the brain stem, consist of clusters of serotonergic (5-HT) neurons that project to almost all regions of the brain. Thus, the RN is an intriguing area for research into the potential effects of SSRIs on myelination and their involvement in a variety of neurological disorders including MDD.

[0011] MicroRNAs (miRNAs) regulate many biological features that might be altered by antidepressants. Two cohorts of chronic unexpected stress (CUS) mouse models for depression underwent behavioral tests for evaluating stress, anxiety, and

depression levels. Following application of the CUS protocol and treatment with the SSRI, citalopram, 48 mice of the second cohort were tested via magnetic resonance imaging and diffusion tensor imaging for differences in brain white matter tracts. RN and superior colliculus were excised from both cohorts and measured for changes in miRNAs, mRNA, and protein levels of candidate genes.

[0012] Using MRI-DTI scans, lower fractional anisotropy and axial diffusivity in brains of stressed mice was found. Moreover, both miR-30b-5p and miR-101a-3p were downregulated in the RN following CUS, and upregulated following CUS and citalopram treatment. The direct binding of these miRNAs to Qki, and the subsequent effects on mRNA and protein levels of myelin basic protein (Mbp), indicated involvement of these miRNAs in myelination ultrastructure processes in the RN, in response to CUS followed by SSRI treatment. According to the present disclosure, SSRIs, and miR-30b-5p and miR-101a-3p are implicated in repairing myelin deficits resulting from chronic stress that leads to depression and other conditions.

[0013] Therefore, based on the foregoing and continuing description, the subject invention in its various embodiments may comprise one or more of the following features in any non-mutually-exclusive combination:

[0014] A method for treating a condition associated with myelin structural deficiencies in a subject, comprising administering to a subject a therapeutically effective amount of a selective serotonin reuptake inhibitor (SSRI).

[0015] A method for treating a condition associated with myelin structural deficiencies in a subject, wherein the SSRI increases expression levels of at least one of miR-30b-5p and miR-101-3p.

[0016] A method for treating a condition associated with myelin structural deficiencies in a subject, wherein miR-30b-5p and miR-101-3p downregulate Qki.

[0017] A method for treating a condition associated with myelin structural deficiencies in a subject, wherein reduced expression of Qki causes increased expression of Myelin Basic Protein (MBP) thereby improving myelin structure in neurons.

[0018] A method for treating a condition associated with myelin structural deficiencies in a subject, wherein miR-30b-5p and miR-101-3p downregulate isoform Qki-5 of Qki.

[0019] A method for treating a condition associated with myelin structural deficiencies in a subject, wherein the SSRI is citalopram.

[0020] A method for treating a condition associated with myelin structural deficiencies in a subject, wherein expression of miR-30b-5p, miR-101-3p, and Qki are restored to normal levels.

[0021] A composition for treating a condition associated with myelin structural deficiencies in a subject, comprising a therapeutically effective amount of SSRI.

[0022] A composition for treating a condition associated with myelin structural deficiencies in a subject, wherein the SSRI is citalopram.

[0023] A method of detecting the presence of a condition characterized by myelin structural deficiencies in a subject comprising obtaining a biological sample from the subject.

[0024] A method of detecting the presence of a condition characterized by myelin structural deficiencies in a subject comprising measuring expression levels of miR-30b-5p and miR-101a-3p in the biological sample.

[0025] A method of detecting the presence of a condition characterized by myelin structural deficiencies in a subject comprising comparing the measured expression levels of miR-30b-5p and miR-101a-3p to a control.

[0026] A method of detecting the presence of a condition characterized by myelin structural deficiencies in a subject, wherein decreased expression levels of miR-30b-5p and miR-101a-3p in the biological sample as compared to the control indicates the presence of the condition.

[0027] A method of detecting the presence of a condition characterized by myelin structural deficiencies in a subject, wherein comparable expression levels of miR-30b-5p and miR-101a-3p in the biological sample as compared to the control indicates the absence of the condition.

[0028] A method of detecting the presence of a condition characterized by myelin structural deficiencies in a subject, wherein the condition is selected from the group consisting of Major Depressive Disorder (MDD), schizophrenia, alcoholism, bipolar disorder, Alzheimer's disease, Parkinson's disease, autism, anorexia, post-traumatic stress disorder (PTSD), addiction, multiple sclerosis, and Generalized Anxiety Disorder (GAD).

[0029] A method of assessing the efficacy of an SSRI treatment in a subject with a condition, the method comprising administering an SSRI to the subject.

[0030] A method of assessing the efficacy of an SSRI treatment in a subject with a condition, the method comprising obtaining a first biological sample from the subject before SSRI administration.

[0031] A method of assessing the efficacy of an SSRI treatment in a subject with a condition, the method comprising obtaining a second biological sample from the subject after SSRI administration.

[0032] A method of assessing the efficacy of an SSRI treatment in a subject with a condition, the method comprising measuring expression levels in the first biological sample and the second biological sample of at least one of miR-30b-5p, miR-101a-3p, and QKI.

[0033] A method of assessing the efficacy of an SSRI treatment in a subject with a condition, the method comprising comparing the expression levels in the first biological sample with expression levels in the second biological sample of at least one of miR-30b-5p, miR-101a-3p, and QKI.

[0034] A method of assessing the efficacy of an SSRI treatment in a subject with a condition, the method wherein increased expression levels of miR-30b-5p and miR-101a-3p in the second biological sample as compared to the first biological sample indicates a therapeutic response to the SSRI treatment.

[0035] A method of assessing the efficacy of an SSRI treatment in a subject with a condition, the method wherein decreased expression levels of Qki in the second biological sample as compared to the first biological sample indicates a therapeutic response to the SSRI treatment.

[0036] A method of assessing the efficacy of an SSRI treatment in a subject with a condition, the method comprising measuring expression levels of miR-30b-5p and miR-101a-3p in the first biological sample and the second biological sample.

[0037] A method of assessing the efficacy of an SSRI treatment in a subject with a condition, the method comprising measuring expression levels of Qki in the first biological sample and the second biological sample.

[0038] A method of assessing the efficacy of an SSRI treatment in a subject with a condition, wherein the SSRI is selected from the group consisting of citalopram, dapoxetine, escitalopram, fluoxetine, fluvoxamine, paroxetine, sertraline, and vortioxetine.

[0039] A method of assessing the efficacy of an SSRI treatment in a subject with a condition, the method, wherein Qki is isoform Qki-5.

[0040] A method of developing therapeutic agents for treating a condition characterized by myelin structural deficiencies in a subject comprising identifying agents that modulate expression levels of at least one of miR-30b-5p, miR-101a-3p, and Qki.

[0041] A method of developing therapeutic agents for treating a condition characterized by myelin structural deficiencies in a subject comprising testing the agents for their ability to increase expression levels of miR-30b-5p and miR-101a-3p in the subject or testing the agents for their ability to decrease expression levels of Qki in the subject.

[0042] A method of developing therapeutic agents for treating a condition characterized by myelin structural deficiencies in a subject comprising selecting agents that either increase expression levels of miR-30b-5p and miR-101a-3p or decrease expression levels of Qki for further development as therapeutic agents.

[0043] A method of developing therapeutic agents for treating a condition characterized by myelin structural deficiencies in a subject, wherein the agents include miRNA mimics.

[0044] A method of developing therapeutic agents for treating a condition characterized by myelin structural deficiencies in a subject, wherein the miRNA mimics downregulate Qki.

[0045] A method of developing therapeutic agents for treating a condition characterized by myelin structural deficiencies in a subject, wherein the agents comprise an Adeno-Associated Virus (AAV), the AAV comprising expression constructs encoding at least one miRNA.

[0046] A method of developing therapeutic agents for treating a condition characterized by myelin structural deficiencies in a subject, wherein the miRNA downregulates Qki.

[0047] A composition for treating a condition characterized by myelin structural deficiencies in a subject comprising an AAV.

[0048] A composition for treating a condition characterized by myelin structural deficiencies in a subject comprising an AAV, the AAV comprising expression constructs encoding at least one of miR-30b-5p and miR-101-3p.

[0049] A composition for treating a condition characterized by myelin structural deficiencies in a subject, wherein the AAV comprises expression constructs of both miR-30b-5p and miR-101-3p.

[0050] A method of treating a condition characterized by myelin structural deficiencies in a subject comprising administering to the subject a therapeutically effective amount of an AAV, the AAV comprising expression constructs encoding at least one of miR-30b-5p and miR-101-3p.

[0051] A method of treating a condition characterized by myelin structural deficiencies in a subject, wherein the administration is performed through stereotactic injection of the AAV into the Raphe Nuclei (RN).

[0052] A method of treating a condition characterized by myelin structural deficiencies in a subject, wherein the stereotactic injection is administered at the following approximate coordinates: anterior-posterior (AP) axis: -4.60.

[0053] A method of treating a condition characterized by myelin structural deficiencies in a subject, wherein the stereotactic injection is administered at the following approximate coordinates: dorso-ventral (DV) axis: -3 relative to the Bregma point and dura mater level.

[0054] A composition for treating a condition characterized by myelin structural deficiencies in a subject comprising a delivery system comprising at least one of encapsulated miR-30b-5p and encapsulated miR-101-3p.

[0055] A composition for treating a condition characterized by myelin structural deficiencies in a subject, wherein the delivery system is suitable for intranasal delivery.

[0056] A method of treating a condition characterized by myelin structural deficiencies, comprising administering a therapeutically effective amount of a composition comprising at least one of encapsulated miR-30b-5p and encapsulated miR-101-3p into the nasal cavity of the subject.

[0057] A method, wherein the condition is Major Depressive Disorder (MDD).

[0058] A method, wherein the condition is schizophrenia.

[0059] A method, wherein the condition is alcoholism.

[0060] A method, wherein the condition is bipolar disorder.

[0061] A method, wherein the condition is Alzheimer's disease.

[0062] A method, wherein the condition is Parkinson's disease.

[0063] A method, wherein the condition is autism.

[0064] A method, wherein the condition is anorexia.

[0065] A method, wherein the condition is post-traumatic stress disorder (PTSD).

[0066] A method, wherein the condition is addiction.

[0067] A method, wherein the condition is multiple sclerosis.

[0068] A method, wherein the condition is Generalized Anxiety Disorder (GAD).

[0069] According to certain non-limiting embodiments, SSRI includes those which can cause increased expression levels of miR-30b-5p or miR-101a-3p. According to some embodiments, the SSRI's include but are not limited to: citalopram, dapoxetine, escitalopram, fluoxetine, fluvoxamine, paroxetine, sertraline, and vortioxetine.

[0070] Additionally, the methods and compositions according to the present disclosure are not limited to application in murine animals but can be applied to all animal models such as in homosapiens and other animal species where increased expression levels of miR-30b-5p and miR-101a-3p leads to decreased expression of Qki and increased expression of Mbp and, ultimately, restoration of myelin deficiencies.

[0071] The present disclosure includes compositions and methods to increase expression levels of miR-30b-5p and miR-101a-3p, or exogenously supply miR-30b-5p and miR-101a-3p or mimics, or downregulation of Qki in the treatment of myelination deficits.

DESCRIPTION OF THE DRAWINGS

[0072] Figure 1: CUS exposed mice display depressive-like and anxiety-like behaviors in the forced swim test (FST) and the elevated plus maze (EPM). (A) latency to immobility and (B) inactive duration in the FST for the first cohort. (C) latency to immobility and (D) inactive duration in the FST for the second cohort. (E) distance moved and (F) duration in the open arms in the EPM for the second cohort. The data are shown as means ± SEM. *p<0.05, **p<0.01, ***p<0.001. Two-way ANOVA test. (A-B) n=5 control, n=6 per each of the other groups. (C-F) n=12 per each of the groups. S, seconds; cm, centimeter.

[0073] Figure 2: Voxel-based analysis of MRI-DTI. (A) MRI-DTI brain FA maps comparing between control and stressed mice (two left brains) and between stressed mice and stressed mice treated with citalopram (two right brains). (B) Analysis of fractional anisotropy between all four groups. (C) MRI-DTI brain AD maps between stressed mice and stressed mice treated with citalopram. (D) Analysis of axial diffusivity between all four groups. (A,C) Statistically significant (p<0.05) clusters are overlaid on coronal maps (posterior to anterior, from left to right). The red-yellow color bar indicates the degree of significance (p-value). (B,D) The data are shown as means ± SEM. *p<0.05, **p<0.01, ***p<0.001. One-way ANOVA test. n=12 per each group.

[0074] Figure 3: miRNA expression analysis following 6 weeks of CUS in mice. Log mean expressions of 302 microRNAs that passed quality control filters of NanoString analysis, compared between (A) the stress/vehicle and the control groups and (B) the stress/citalopram and the stress/vehicle groups. Each dot represents a specific miRNA. Red dots represent miRNA with significant downregulated differential expression. Blue dots represent miRNA with significant upregulated differential expression. (C) Real-time qPCR analysis of miR-30b-5p and miR-101a-3p. (C) The data

are shown as means ± SEM. *p<0.05, ***p<0.001. One-way ANOVA. (A-B) n=3 per each mouse group, (C) n=5 control, n=6 per each of the other mouse groups.

[0075] Figure 4: miR-30b-5p and miR-101a-3p directly regulate Qki mRNA. (A) Qki expression profile assessed by RT-qPCR. Significantly increased expression levels of Qki mRNA in RN of stressed mice compared to stressed and treated mice. (B) Real-time PCR analysis of miRNA following two repeated 24h transfections and of (C) QKI mRNA expression following 72h of the indicated miRNA transfection relative to a control plasmid transfection, in the SH-SY5Y cell line. (D) Sequences of the mature miR-30b-5p and miR-101a-3p and the Renilla/firefly luciferase psiCHECK2 constructs (WT and mutant) under the regulation of QKI 3'UTR, around the miR-30b-5p and miR-101a-3p binding sites. The miR-mRNA binding sites are shown in bold. Mutated nucleotides are shown in red. (E) Significantly higher luciferase activity levels of the mutated QKI 3'UTR construct, 72h following transfection with miR-30b-5p or miR-101a-3p in HEK-293T cells, compared to the activity levels of the WT luciferase construct. The data are shown as means ± SEM. *p<0.05, **p<0.01, ***p<0.001. (A) One-way ANOVA (B-D) Two-tailed Student's t-test. (A) n=5 control, n=6 per each of the other mouse groups (B-D) n=3. WT, wild type. Mut, Mutant.

[0076] Figure 5: Qki and Mbp expression in raphe nuclei (RN) tissue following 6 weeks of CUS in mice. (A) Real-time qPCR analysis of Qki and Mbp mRNA in RN tissues from the four mice groups. (B) Western blot analysis of QKI and MBP protein in all four mice groups. The quantification was done upon normalization to Tubulin housekeeping protein expression. (C) Western blots of MBP and QKI isoform expression levels in the RN of control mice, stressed mice, and treated mice (both control and stressed). (D) Expression levels of Qki-5 and (E) Qki-7 isoforms in all four mice groups following PCR amplification. The data are shown as means ± SEM. *p<0.05, **p<0.01, ***p<0.001, ****p<0.0001. One-way ANOVA test. (A, D-E) n=5 control, n=6 per each of the other groups. (B) n=9 per each group.

[0077] Figure 6: CUS mice showed impaired myelin ultrastructure. (A) The g-ratio of myelinated axons in the RN of the four mice groups. (B) Representative images of myelin ultrastructure in the RN of the four groups. Scale bars: upper= 5 µm; middle=

500 nm; lower= 100 nm. ****p<0.0001. One-way ANOVA. A. n=203 axons from two control mice, n=285 axons from three control mice treated with citalopram, n=216 axons from two stressed mice, n=274 axons from three stressed mice treated with citalopram.

[0078] Figure 7: A model depicting the role of miR-30b-5p and miR-101a-3p, and their target gene Qki, in the mode of action of SSRIs in MDD. (A) Under CUS conditions for 6 weeks, miR-30b-5p and miR-101a-3p are downregulated in the RN. This results in higher expression of Qki, which in turn causes lower levels of Mbp mRNA and protein. This causes looser compacting of myelin sheaths of RN neurons. (B) Under CUS conditions for 6 weeks and citalopram treatment for 3 weeks, miR-30b-5p and miR-101a-3p are up-regulated in the RN, resulting in lower expression of Qki. This in turn causes higher levels of Mbp mRNA and protein. The latter results in denser and correct compacting of myelin sheaths of RN neurons.

DETAILED DESCRIPTION

[0079] The present disclosure examines the effects of SSRIs, specifically citalopram, on microRNA and gene expression of RN of stressed mice. The findings show that chronic stress causes depressive-like symptoms in mice, and alters expression levels of two microRNAs, miR-30b-5p and miR-101-3p, along with their target gene, Qki, which subsequently affects Myelin Basic Protein (MBP) expression and myelin structure. Furthermore, it was identified that these depressive symptoms and molecular changes are ameliorated by citalopram treatment specifically due to its effect of increasing the expression levels of miR-30b-5p and miR-101-3p. Importantly, the present disclosure demonstrates that depressive symptoms involve changes in myelin structure, and that citalopram does not merely block SERT reuptake, it restores normal myelin structure by increasing expression levels of miR-30b-5p and miR-101-3p.

[0080] According to certain embodiments, the present disclosure relates to a composition and method of treating myelin structural deficiencies and restoring normal myelin structure through treatment with SSRIs such as citalopram to increase expression of miR-30b-5p and miR-101-3p.

[0081] In other embodiments, the present disclosure relates to a composition and method of treating myelin structural deficiencies and restoring normal myelin structure through supplementation of miR-30b-5p and miR-101-3p, such as through administration of an Adeno-Associated Virus (AAV) containing said microRNAs or expression constructs encoding said microRNAs.

[0082] According to other embodiments, the disclosure relates to intranasal delivery of encapsulated miR-30b-5p and miR-101-3p. Intranasal delivery represents a promising approach for non-invasive gene therapy and treatment of neurological disorders. This method involves administering miR-30b-5p and miR-101-3p encapsulated in nanoparticles or other delivery vehicles directly into the nasal cavity. The nasal route provides a direct pathway to the central nervous system (CNS) via the olfactory and trigeminal nerves, allowing for efficient delivery of therapeutic agents to the brain. Encapsulation enhances the stability and bioavailability of miR-30b-5p and miR-101-3p, protecting them from degradation in the nasal mucosa and improving its uptake by target cells. This technique is particularly advantageous for targeting CNS disorders, as it bypasses the blood-brain barrier and provides a more localized treatment compared to systemic administration. Intranasal delivery of encapsulated miR-30b-5p and miR-101-3p provides a non-invasive treatment method for the treatment of myelin structural deficiencies to restore normal myelin structure.

[0083] According to some embodiments, the disclosed miRNAs can be encapsulated within various delivery systems for therapeutic administration. These delivery systems include, but are not limited to, liposomes, polymer-based nanoparticles (such as PLGA and chitosan), inorganic nanoparticles (including gold, silica, and iron oxide), exosomes, and cell-penetrating peptides. These encapsulation methods protect the miRNAs from degradation, facilitate cellular uptake, and can be engineered for targeted delivery, thereby enhancing the therapeutic potential of the claimed miRNAs.

[0084] While the disclosure includes discussion and examples of mice to illustrate the effects of citalopram on miR-30b-5p and miR-101-3p, the methods and compositions described herein are not limited to murine models. The findings and therapeutic approaches including compositions and methods outlined herein are broadly

applicable to humans and other animal models. The principles contained herein, including citalopram-induced modulation of miRNA expression levels, upregulation or supplemental expression of miR-30b-5p and miR-101-3p, and administration of miR-30b-5p and miR-101-3p through AAV or intranasal delivery of encapsulated miRNAs are expected to be relevant across various species due to the conserved nature of these miRNAs and their associated pathways in mammalian physiology. Thus, the present disclosure includes applications of such compositions and methods to achieve similar effects in human subjects as well as in other animal models, such as non-human primates, rats, and other mammalian species. This broader applicability underscores the potential of these methods and compositions to be used in diverse therapeutic contexts and across different biological systems.

[0085] 1. Animals, treatment and CUS

[0086] A total of 23 male C57BL/6, 6 weeks old mice were tested in the first cohort experiment, and 48 male C57BL/6, 6 weeks old mice were tested in the second cohort. Male mice were used in order to avoid effect of female hormonal cycles on the results. The experiment was designed where in the 1st cohort, 6 mice were subjected to Chronic Unpredictable Stress (CUS) and given water, 6 mice exposed to CUS and given citalopram hydrobromide (10mg/kg/day) in drinking water (0.1mg/ml), 6 mice were given citalopram in drinking water and 5 mice were used as controls and given water. In the second cohort, 12 CUS-exposed mice were given vehicle via i.p. injection, 12 mice exposed to CUS were given citalopram hydrobromide (10mg/kg/day) (C7861) via i.p. injection, 12 mice were given citalopram via i.p. injection and 12 mice were used as controls and given vehicle via i.p. injection.

[0087] CUS protocols entailed a randomized six-week schedule of daily mild stressors, which started when mice were 6 weeks old. Treatment (vehicle or citalopram) was given at the start of the fourth week (i.e. mice were 9 weeks old), for three weeks. Additionally, mice were weighed on the first day of each of the six weeks of CUS and nestlet measurements were made on the days following a “change to new cage” stressor.

[0088] Every mouse in a given cohort in the CUS groups, was exposed to the same stressor on a given day. Stressful stimuli were administered at a random time of day, though always during the light portion of the controlled light/dark cycle. Following six weeks of CUS exposure, behavioral tests were performed to quantify the effects of this stress.

[0089] Each stressed mouse was housed individually, while control mice were group housed and remained in their home cages throughout, in the Vanderbilt Murine Neurobehavioral Core during the first cohort, or in the conventional murine center at the Faculty of medicine at Tel Aviv University during the second cohort, with controlled 12-hour light/dark cycles, freely available food and water, and controlled temperature and humidity. All experimental procedures were approved by the Vanderbilt Institutional Animal Care and Use Committee under the protocol M/15/014, or by the Tel Aviv University Institutional Animal Care and Use Committee under the protocol TAU-MD-IL-2206-167-5.

[0090] 2. Stressors

[0091] Each day was randomly assigned one of six possible stressors or as a rest day (no stressor).

[0092] 1. Changing to a New Cage. This stressor consisted of removing a mouse from its home cage and rehousing it in a new, clean cage. No bedding, food or water was carried over to the new housing. A nestlet was placed in the new cage.

[0093] 2. Confinement to Plastic Cylinder. This stressor consisted of removing the mouse from its home cage and placing it in a restraint tube for 5 minutes. After the period of confinement, the mouse was returned to its unaltered home cage.

[0094] 3. Shaking of Home Cage. This stressor consisted of shaking the mouse home cage three times by hand for a duration of thirty seconds each, with a one-minute interval between each shaking. The home cage is shaken with enough force so that the mouse displays tonic immobility.

[0095] 4. Exposure to Water. Each mouse was removed from its home cage and placed in a 500ml beaker containing 1cm of water at room temperature for 6 minutes. Mice were hand-dried and returned to their home cage.

[0096] 5. Swapping Home Cage of Two Mice. This stressor consisted of removing two mice from their respective home cages and rehousing them in each other's home cages. No bedding, food or water were replaced or swapped between cages. Mice remained in their new home cage until the next cage swap stimulus, or until the conclusion of the six weeks of CUS.

[0097] 6. Tilt cage. In this stressor mice remained in their respective cages while cages were tilted to 45° for a duration of two hours.

[0098] 7. Rest day. No stress stimulus was administered. Mice remained in their unaltered home cages.

[0099] 3. Behavioral testing

[0100] Animals were tested during the light phase and acclimated to testing room conditions for 30 minutes. All apparatuses were cleaned with chlorine dioxide disinfectant prior to the first testing session and between sessions. Mice were tested in a randomized order for each test. Test order was designed to minimize carryover anxiety on subsequent assays. Individual tests were conducted with a minimum of 24 hours between each test.

[0101] 3.1 Forced Swim Test (FST)

[0102] The forced swim test is used to evaluate depressive like behavior. The apparatus is a clear Plexiglas cylinder, 24 cm high and 19 cm in diameter, filled with approximately 16 cm of water at 23°C. In the test, the mouse was placed in the cylinder for 7 minutes and then moved to a heated cage until the fur dried completely. Typically, the mouse gradually stopped swimming before being removed. Water was changed and the apparatus cleaned between each test. Immobility duration, the time the mouse remained floating motionless was measured during the last five minutes. All tests were filmed by video camera. A blind competent observer scored immobility for the first

cohort, while the second cohort was tracked and analyzed using EthoVision XT™. Latency to first immobile period and total immobility were recorded.

[0103] 3.2. Elevated Plus Maze (EPM)

[0104] The elevated plus maze is used to evaluate anxiety like behavior. The apparatus consists of a four-armed platform (+ shape) elevated 40 cm off the ground. Two arms are "closed" and confined by walls (15 cm high) and two arms are "open" with no walls. Each arm is 35 cm long and 5 cm wide, and similar arms face one another. In the test, each mouse is placed at the center of the EPM facing toward one of the closed arms and then allowed to move freely for 7 minutes. When the mice are placed on the maze, the video-tracking system starts. The respective number of entries into the open and closed arms and the time spent exploring each arm are recorded for each mouse. After 7 minutes of testing, mice were removed from the plus maze and placed back in their home cage outside the testing environment. The EPM was cleaned with Virusolve+™ before the next test.

[0105] 4. Magnetic Resonance Imaging (MRI) and Diffusion Tensor Imaging (DTI)

[0106] Forty-eight twelve-week-old mice underwent MRI-DTI scans. During MRI sessions, anesthesia was induced and maintained using isoflurane (1.5%) in pure oxygen. A heating system was used to maintain the animal body temperature, and their respiration was monitored and maintained at 30–50 breaths/min using a pneumatic balloon positioned against the animal's chest.

[0107] MRI was performed in the Strauss computational neuroimaging center at Tel Aviv University, by a scanner equipped with a 660mT/m gradient unit, using a cross-coil configuration of 86 mm transmissive Volume coil and mouse quadrature coil as a receiver. The MRI scan protocol included structural T2 weighted (T2w) images that were acquired with the rapid acquisition with relaxation enhancement sequence (RARE) and Diffusion Tensor Imaging (DTI) acquisition with a Diffusion-Weighted Spin-Echo Echo-Planar-Imaging pulse sequence (DW-SE-EPI). T2w acquisition was done with the

following parameters: TR=2500 ms; effective TE: 30 ms, RARE factor 8 with 8 repetitions. 20 coronal slices, 0.6 mm thick (no gaps), with in-plane resolution of 0.1 mm2 covering the entire brain, and lasts 4:00 min. For DTI we have used TR/TE=3000/22.3 ms, Δ/δ=10/2.5 ms, 2 EPI segment, 30 gradient directions with b-value at 1000 s/mm2 and three B0 images. 28 axial slices, 0.6 mm thick (no gaps), with in-plane resolution of 0.175 mm2. The DTI acquisition took 10:00 min.

[0108] DTI dataset was corrected for head movement and eddy current distortion using ExploreDTI™ platform within MATLAB™. Following the corrections, the dataset underwent non-linear tensor estimation with structural corrections to the anatomical T2w image. Several indices were extracted from DTI analysis, such as fractional anisotropy (FA), mean diffusivity (MD), and axial and radial diffusivities (AD and RD, respectively) that were then co-registered and normalized to a template mouse brain using Statistical Parametric Mapping 12. An ANOVA test was performed based on DTI indices between four groups of mice, where differences lower than alpha of 0.05 were considered significant. The p values were then plotted upon the template brain.

[0109] 5. Tissue collection

[0110] For RNA extraction and western blotting experiments, mice were euthanized by rapid decapitation without anesthesia. For TEM experiments, mice were perfused according to TEM protocol (see section 14). Brains were harvested and midbrains were dissected by coronal sectioning of the brain at Bregma -4.24 mm and -5.02 mm. Superior colliculus and raphe-enriched sections were separated by making an incision at the aqueduct (Interaural 3.44 mm), where the tissue below the aqueduct was considered enriched in serotonergic cell bodies. Samples aimed for RNA extraction and western blotting experiments were snap frozen in liquid nitrogen, while samples for TEM or immunofluorescence experiments were kept in 4°C according to TEM protocol.

[0111] 6. RNA extraction

[0112] Twenty-three samples from the 1st cohort underwent RNA purification using phenol-chloroform extraction: Tissue samples were first homogenized with

stainless steel beads and then lysed using TRIzol™ reagent, followed by RNA separation using chloroform and isopropanol precipitation. The final RNA concentrations and purity were measured using a NanoDrop™ ND-1000 spectrophotometer.

[0113] 7. miRNA profiling

[0114] The multiplexed NanoString™ nCounter miRNA expression assay was used to profile ~800 mice miRNAs (according to the established miRNAs in the array) in the RN and SC derived RNA samples. The assay was performed according to the manufacturer's protocol. Analysis included adjustment of p-values for genome-wide miRNA profiling, in order to prevent inflation of the false positive rate in multiple testing.

[0115] 8. Reverse Transcription (RT)-PCR

[0116] Reverse transcription reactions for mRNA and for specific mature miRNAs were performed using the High-Capacity cDNA Reverse-Transcription Kit with random primers or TaqMan™ miRNA assays, respectively, according to the manufacturer's recommendations.

[0117] 9. Polymerase Chain Reaction (PCR)

[0118] Amplification of specific mRNA regions was performed using cDNA, by Polymerase Chain Reaction (PCR), using KAPA2G Fast HotStart ReadyMix™ and custom planned primers (Supplementary table 1). PCR products were loaded and run through a 1.5% agarose gel. Bands signal was detected via FluorChem M™ camera and analyzed using ImageJ™ software.

[0119] 10. Real-time quantitative PCR

[0120] Real-time polymerase chain reaction (PCR) was performed to validate top significant candidates obtained by mRNA sequencing and the NanoString nCounter miRNA assay™, according to the manufacturer's instructions. MiRNA and mRNA expression was tested using TaqMan universal PCR Master Mix™ and Quanta qPCR Gene Expression Master Mix™, respectively. PCR amplification and analysis were performed using the StepOne Real-Time PCR System™. Comparative critical threshold

(Ct) values, obtained by real-time PCR analysis, were used for relative quantification of gene or miRNA expression, and determination of the fold-change of expression. Fold change values were obtained by using the formula: $2^{-\Delta\Delta Ct}$ (70). Normalization for miRNA and mRNAs was performed compared to mouse SnoRNA202 and mouse Gapdh expression, respectively, which expression was stable across all groups (supplementary tables 2&3).

[0121] 11. miRNA transfection

[0122] For miRNA transfection experiments, SH-SY5Y (human bone marrow-derived neuroblastoma) cells were seeded in 24-well plates at a concentration of 8×104 cells/well and transfected with 500 ng of miRVec-30b-5p, miRVec-101a-3p or an empty vector. Transfections were performed in triplicate using Lipofectamine 2000 transfection reagent™ according to the manufacturer's instructions. RNA was extracted following 48h for miRNAs and following 72h for mRNAs. Transfection efficiencies were measured by GFP fluorescence in all cells, indicating a transfection efficiency of >20%.

[0123] 12. Dual luciferase reporter assays

[0124] Fragments of ~700 bp from QKI 3′UTR, spanning the presumed miRNA-binding sites, were cloned, downstream of the Renilla luciferase reporter under the control of T7 promoter of the psiCHECK-2 plasmid, which also contains a firefly luciferase reporter (used as a control) under the HSV-TK promoter. The negative controls of QKI, in which miRNA-mRNA binding is abolished, were generated by mutating three nucleotides in the seed binding region of the cloned QKI 3'UTR, using the QuikChange Lightning Site-Directed Mutagenesis Kit™. For luciferase assays, HEK-293T human cells were transfected using Lipofectamine 2000 transfection reagent. Next, the cells were transfected with 5 ng of psiCHECK-2 plasmid containing the desired 3′UTR, with or without site-directed mutations, and 485 ng miRVec containing the desired pre-miRNA or an empty vector. At 72h following transfection, firefly and Renilla luciferase activities were measured using the Dual Luciferase Reporter assay system kit™ and the LUMIstar Omega Luminometer™, according to the manufacturer's

recommendations. Renilla luciferase results were normalized to the values of the firefly luciferase. Significant results represent 3 biological replicates.

[0125] 13. Western blotting

[0126] Raphe nuclei and superior colliculus samples from the 2nd cohort were homogenized in solubilization buffer (50 nM HEPES PH=7.5, 10 nM NaCl, 10% glycerol, 1% Triton x-100, 1 mM EDTA pH = 8, 1 mM EGTA pH = 8, 1.5 mM MgCl2, 200 µM Na3VO4, and protease inhibitor cocktail 1 diluted 1:100). Equal amounts of protein from each sample were loaded and resolved by SDS–polyacrylamide gel electrophoresis through 12.5% gel. The gel was electrophoretically transferred to a nitrocellulose membrane in transfer buffer (25 mM Tris, 190 mM glycine, and 10% methanol absolute). Membranes were blocked for 45 min in TBST buffer (0.05 M Tris HCl pH = 7.5, 0.15 M NaCl, and 0.1% Tween 20) with 6% skimmed milk, and blotted overnight with rat anti-MBP antibody (MAB386), rabbit anti-β-Tubulin (AB108342) and mouse anti-QKI (MA5-27651) in TBST buffer, followed by a secondary antibody linked to horseradish peroxidase, goat anti-rat, goat anti-rabbit, and goat anti-mouse respectively (AP136P, AP132P, AP130P, Sigma-Aldrich™). Immunoreactive bands were detected with the enhanced chemiluminescence reagent.

[0127] 14. Transmission electron microscopy (TEM)

[0128] Twelve-weeks-old mice from the 2nd cohort were deeply anesthetized with isoflurane, transcardially perfused with 15 ml ice-cold PBS solution followed by 15 ml fresh ice-cold fixative solution containing 2.5% glutaraldehyde (G5882) + 2% PFA (EMS, PA, USA) in 0.1 M sodium cacodylate buffer (pH 7.4) (C0250). Brains were dissected and Raphe nuclei areas were kept in the fixation solution overnight at 4°C and then moved to a solution containing 2.5% glutaraldehyde, 0.1M cacodylate buffer and Phosphate-buffered saline (PBS). After several washings in PBS, brain tissues were post fixed in 1% osmium tetroxide (OsO4) in PBS for 2 hours at 4°C. Dehydration was carried out in graded ethanol solutions (10 min each; 50, 70, 90 and 2 × 10 min 100%) and embedding in Glycid ether. Ultra-thin sections (approximately 70 nm) were cut,

stained with uranyl acetate and lead citrate, mounted on Formvar/Carbon coated grids and were examined in Jeol™ 1200EX transmission electron microscope. For quantifying the number of myelinated axons and characterize the g-ratio, ten images were taken from each of three different locations, to cover multiple regions of the Raphe nuclei. For quantifying the g-ratio, approximately 100 myelinated axons per mouse were analyzed, by manually measuring the ratios of the axons diameter and the myelinated axons diameter.

[0129] 15. Statistical analysis

[0130] All data was analyzed using GraphPad Prism software v.9. Normality of data distribution was evaluated using the Shapiro-Wilk test; Outliers were detected by the Grubbs test. For behavioral data, each experimental cohort was analyzed independently, as soon as behavioral measurements were finished, to assess effects of treatment and stress. The contribution of stress and citalopram treatment was analyzed using a two-way ANOVA and Tukey corrections for multiple testing between categories. Continuous variables between two groups were analyzed by the Student's t-test. Continuous variables between more than two groups were analyzed by the One- or Two-way ANOVA tests. P-values < 0.05 were considered significant.

[0131] Results

[0132] Stress and citalopram affect behavior in CUS mice

[0133] The first cohort consisted of male C57BL/6 mice (aged 6 weeks at the start) exposed to CUS in order to impose alterations in depressive and anxiety behaviors. These behaviors were measured by the forced swim test (FST). CUS induced a significant decrease in the latency to immobility. These effects were modified by citalopram dosing (Figure 1A). Two-way ANOVA analysis of the behavioral data revealed significant interaction effects in latency to immobility ($F(1,19)=9.86$, $p=0.005$) and significant effects of CUS ($F(1,19)=16.89$, $p=0.0006$) and treatment ($F(1,19)=4.45$, $p=0.048$). Significant differences were found between the control group and all the other groups (control/vehicle; $p=0.008$, stress/vehicle; $p=0.0004$ and stress/treatment;

p=0.002), though stress/vehicle and stress/treatment groups did not differ significantly. Significant differences were not observed in the total inactive time across the four groups (Figure 1B).

[0134] Based on the trend seen in the first cohort, a second, larger cohort was established, which also consisted of 6-week-old mice exposed to CUS, citalopram or both, for 6 weeks. Alterations in depressive and anxiety behaviors in this cohort were measured by the FST and the elevated plus maze (EPM) tests. Two-way ANOVA analysis of the FST behavioral data revealed a significant effect of treatment on latency to immobility ($F(1,43)=4.24$, $p=0.045$), and CUS induced a decrease in latency to immobility (Figure 1C). Two-way ANOVA analysis of the behavioral data revealed interaction effects in the total inactive time ($F(1,43)=5.81$, $p=0.020$) and an effect of treatment on the total inactive time ($F(1,43)=4.42$, $p=0.041$). Specifically, the inactive duration was increased in the stress/vehicle group compared to the stress/treatment group ($p=0.016$) (Figure 1D). Two-way ANOVA analysis of the EPM behavioral data revealed significant interaction effects on the total distance moved ($F(1,43)=13.82$, $p=0.0006$); a larger distance was moved in the stress/treatment group than in the stress/vehicle group ($p=0.001$) (Figure 1E). Analysis of the time in the EPM open arms revealed significant interaction effects ($F(1,43)=7.152$, $p=0.010$); the time in open arms was lower in the stress/vehicle group than in the control/vehicle or stress/treatment groups ($p=0.001$ and $p=0.021$, respectively) (Figure 1F). Both FST and EPM indicated that citalopram attenuated the effects of CUS.

[0135] Stress and citalopram affect brain diffusivity

[0136] To examine changes in brain white matter we used MRI-DTI scans. This revealed lower FA in stressed mice than in control mice or stressed mice treated with citalopram. These results indicate axonal degeneration, demyelination or less dense axonal packing in stressed mice brains. Comparing control and stressed mice (Figure 2) showed a significant ($p<0.05$) effect of stress on FA in five regions, including the RN area (-28%), brain stem area (-19%), retro-spinal cortex (-30%), corpus callosum (-24%) and caudate-putamen (-23%). Comparing stressed mice to stressed mice treated with

citalopram (Figure 3B) showed a significant ($p<0.05$) effect of stress in six regions, including the RN area (-30%), brain stem area (-21%), corpus callosum (-23%), caudate-putamen (-28%), dentate gyrus (-32%) and globus pallidus (-24%).

[0137] MRI-DTI also revealed lower axonal diffusivity in stressed mice than in stressed mice treated with citalopram (Figure 2D), indicating axonal injury. The effect of stress was significant ($p<0.05$) in three regions, including the RN area (-12%), thalamus (-13%) and caudate-putamen (-13%).

[0138] T2 relaxation images were used to assess volumetric changes in the brain following stress or citalopram treatment. Neither of them significantly affected the examined brain region volumes.

[0139] Stress and citalopram alter miR-30b-5p and miR-101a-3p expression in the raphe nucleus

[0140] As the disclosers were interested in changes in the serotonergic center of the brain, twelve RN and twelve superior colliculus (SC, i.e. control area) RNA samples from the first cohort were sent for miRNA profiling via the NanoString platform™. Principal component analysis (PCA) was used to assess whether global miRNA expression can distinguish between the four mouse groups in each tissue. PCA for SC revealed no distinction between the groups. However, PCA for RN distinguished stress/citalopram samples from the other groups; and mildly distinguished between the three other groups. To evaluate whether a miRNA-based risk classifier pattern can be identified, miRNA expression between the groups (control vs. stress, stress vs. stress/ citalopram) was compared. Many miRNAs were differentially expressed between the groups; and for several miRNAs whose responses to stress and to stress/citalopram were inversely correlated, statistical significance ($p<0.05$) was shown (Figure 3A, 3B). The two miRNAs (miR-30b-5p and miR-101a-3p) with the most significant change were selected for further evaluation.

[0141] Real-time PCR was conducted to validate the results, utilizing 11 additional samples from the first cohort that had not been analyzed by the NanoString

assay. One-way ANOVA analysis for miR-30b-5p and miR-101a-3p verified that these miRNAs demonstrated the same trend as seen in the NanoString assay: reduced expression following stress and increased expression following stress and citalopram treatment (miR-101a-3p, p=0.020, and miR-30b-5p, p=0.026) (Figure 4C).

[0142] miR-30b-5p and miR-101a-3p target Qki

[0143] Next, the disclosers searched for mouse genes that were targeted by both miRNAs. For this purpose, the disclosers considered genes as miRNA targets predicted as a target-gene by at least three of four prediction tools: Target Scan, Diana, miRDIP and Pita. This resulted in four target-genes for both miR-30b-5p and miR-101a-3p: Cpeb3, Fndc3a, Edem3 and Qki. The expression levels of the mRNAs of all four genes were tested in the RN tissue by qPCR. Cpeb3, Fndc3a and Edem3 showed no significant change. Only Qki showed an effect of treatment (p=0.0006); expression levels were inversely correlated with miRNAs in both the stress and stress/citalopram groups (p=0.0003) (Figure 4A).

[0144] To validate the predicted interaction of miR-30b-5p or miR-101a-3p with Qki, the disclosers quantified the levels of the relevant mRNA after transfection of each miRNA. Two miRNA vectors that expressed miRNA of miR-30b-5p or miR-101a-3p were transfected into the SH-SY5Y cell line for 72 hours. Real-time PCR reactions that were carried out on each transfectant revealed the three-fold overexpression of miR-30b-5p, and the 1.5-fold overexpression of miR-101a-3p (p=0.006 and p=0.040, respectively, Figure 4B). Further, overexpression of miR-30b-5p and miR-101a-3p reduced Qki levels by 23% and 12%, respectively (p=0.014 and p=0.030, respectively, Figure 4C).

[0145] To demonstrate the direct functional regulation and binding of miR-30b-5p or miR-101a-3p to Qki, a luciferase reporter assay was conducted. Negative controls were generated by performing site-directed mutagenesis reactions that resulted in changes of three nucleotides of the respective 3′UTR miRNA-binding sites of Qki in the seed region (Figure 4D). After 72 hours of co-transfection of Qki 3'UTR construct and

miRNA vector plasmid in HEK-293T cells, Renilla luciferase and firefly luciferase expression was measured. Figure 4E shows that transfection of plasmids containing the wild-type 3′UTR of Qki resulted in lower luciferase activity than that observed following transfection of plasmids containing the mutant 3′ UTR (luciferase activity was reduced to 0.66 and 0.63 relative to mutant levels, by miR-30b-5p and miR-101a-3p, p=0.004 and p=0.013, respectively).

[0146] Correlation between Qki and Mbp in the mouse raphe nucleus

[0147] As Qki is expressed in oligodendrocytes and involved in myelination processes and their maintenance, we looked for myelin-related genes that might be affected by Qki. The tested genes were Cnp, Plp1, Mag and Mbp. Cnp, Plp1 and Mag and showed no significant effect of CUS. In contrast, myelin basic protein (Mbp) showed significantly decreased mRNA expression levels in the stress condition, and increased levels in the stress and treatment condition (p=0.001). The expression levels of Mbp were inversely correlated to Qki (stress/vehicle Qki vs. Mbp; p<0.0001) (Figure 5A).

[0148] Thirty-six samples from the second cohort were used to investigate changes in protein levels. Compared to stressed mice that were not treated with citalopram, stressed mice that were treated showed significantly lower (p=0.044) QKI protein expression (Figure 5B). Although not significant (p=0.209), the opposite trend was shown for MBP protein expression, namely lower expression following stress, and higher expression following citalopram treatment.

[0149] There is notable involvement of the nucleic isoform of Qki, which includes exon 8 (Qki-5), in affecting levels of Mbp in oligodendrocytes. Therefore, the disclosers tested the level of this isoform in the samples. Although not statistically significant, a trend was seen by which levels of Qki-5 were higher in stressed mice, and lower in stressed mice treated with citalopram (Figure 5D). To ensure that these changes were specific for the Qki-5 isoform, levels of the cytoplasmic isoform Qki-7 (which includes exon 7) were tested as well. The level of Qki-7 was higher in control mice than in control

mice treated with citalopram (p=0.034); however, Qki-7 levels were similar between stressed mice and stressed mice treated with citalopram (Figure 5E).

[0150] Unchanged mRNA or protein levels in the mouse superior colliculus (SC)

[0151] Following the original NanoString analysis, which showed no change in miRNA expression following stress or citalopram treatment in the SC tissue, the disclosers sought to examine mRNA and protein expression for Qki and Mbp. SC tissue from stressed mice showed similar mRNA and protein expression levels of Qki and Mbp to those of control mice. SC tissue from stressed mice treated with citalopram showed similar expression levels of Mbp mRNA and protein to those of control mice. Qki mRNA expression was significantly higher in the stressed mice than in the stressed mice that were treated (p=0.020). However, no such difference was observed in the expression of Mbp mRNA, or in QKI and MBP proteins.

[0152] CUS impairs myelin ultrastructure

[0153] Next, it was investigated whether the abovementioned molecular deficits affect myelin structure in CUS mice. Analysis of myelin ultrastructure (Figure 6A) revealed a significantly decreased g-ratio, a parameter used for assessment of axonal myelination, for stressed mice compared to control mice, and compared to stressed mice treated with citalopram ($p<0.0001$ for both comparisons). This indicates increased myelin thickness in stressed mice. However, in images of the axon ultrastructure (Figure 6B), the myelin diameter of axons of stressed mice was not thicker. Notably, the myelin sheaths in these axons were less compressed together, with gaps formed between them. Citalopram treatment restored normal compacting of the myelin sheaths.

[0154] Expression of miR-30b-5p and miR-101-3p with Administration of Adeno Associated Virus

[0155] In certain experiments, mice can be administered stereotactic injections of AAV's containing at least one of miR-30b-5p and miR-101-3p or expression constructs encoding at least one of these miRNAs. First, mice can be injected with an AAV containing the Qki gene to show that overexpression of Qki results in damaged myelin

in the RN, which in turn results in MDD. Next, mice can be administered AAV's containing at least one of miR-30b-5p and miR-101-3p, or both, or expression constructs encoding at least one, or both, to demonstrate their efficacy as a treatment. All injections can be to the Raphe nucleus, in the following coordinates: anterior-posterior (AP) axis: -4.60, dorso-ventral (DV) axis: -3 (relative to the Bregma point and dura mater level). Once reaching the DV coordinates, the needle can then be withdrawn 0.15 mm to create room for the liquid to be injected into. Results from the expression of miR-30b-5p and miR-101-3p achieved through AAV administration can be used to complement the data showing that citalopram-induced increases of miR-30b-5p and miR-101-3p cause decreased expression of Qki, increased expression of Mbp, and restoration of myelin structural deficiencies and normal compacting of myelin sheaths.

[0156] Discussion

[0157] Chronic stress is well-established as a common trigger for the onset of depressive symptoms, via its effect on the hypothalamic pituitary adrenal axis. Chronic stress can also lead to changes in brain function and morphology, which are neurological aspects of MDD that are not easily accessible for molecular studies in living humans. Abundant studies in both humans and rodents showed that miRNA expression profiles are altered during chronic stress, and that dysregulation of their levels may affect the expression of genes related to the etiology of MDD.

[0158] Behavioral tests showed that the CUS protocol applied here resulted in mice that presented depressive-like symptoms, and citalopram alleviated these symptoms. MRI-DTI scans showed decreases in FA and axonal diffusivity in brains of stressed mice, in areas that included the RN, brain stem, corpus callosum, caudate putamen and thalamus. These changes suggest axonal degeneration, demyelination or less dense axonal packing in brains of chronically stressed mice. The present disclosure demonstrates the importance of the RN in the etiology of MDD, the effects of chronic stress on CNS myelin structure, and the tentative role of SSRI treatment and miR-30b-5p and miR-101a-3p modulation in correcting these effects. The disclosed

findings have broad implications for the treatment of other neurological disorders involving myelin deficiencies.

[0159] Using global miRNA expression analysis, several miRNAs were identified that were differentially expressed between the stress and stress/citalopram groups, while some miRNAs had an inversely correlated response to stress and to stress/citalopram. Two miRNAs, miR-30b-5p and miR-101a-3p, exhibited the most significant reduced expression. This was validated in all the RN samples by real-time qPCR. These findings emphasize that CUS can alter the expression levels of miRNAs in the RN, and that SSRI treatment, such as citalopram, can restore RN expression of these miRNAs to normal levels and that restoration of miR-30b-5p and miR-101a-3p to normal levels is an effective treatment for neurological disorders involving myelin deficiencies.

[0160] Most importantly, miR-101a-3p was downregulated in the total plasma of individuals with MDD compared with controls. This suggests the involvement of miR-101a-3p in MDD pathophysiology. These results suggest that miR-101a-3p levels are down-regulated following chronic stress and are upregulated and restored to normal levels following citalopram treatment.

[0161] Four protein coding mouse genes were identified that are regulated by both miR-30b-5p and miR-101a-3p, namely: *Cpeb3*, *Fndc3a*, *Edem3* and *Qki*. Only one of them, *Qki*, was inversely correlated to both miRNAs under both the stress and the stress/citalopram conditions. *Qki* (quaking gene) is highly expressed in brain tissue and is involved in oligodendrocyte and myelination processes. A specific known mutation in this gene results in severe deficits in myelin, a deficiency that is more pronounced in the brain than in the spinal cord or the peripheral nervous system. *Qki* is an RNA-binding protein with a number of isomers, which regulates pre-mRNA splicing, export of mRNAs from the nucleus, protein translation and mRNA stability. *Qki* was shown to affect RNA processing of the genes encoding *Mbp* and *Mag* in oligodendrocytes.

[0162] Using luciferase assays revealed the direct regulation of *Qki* by both miR-30-5p and miR-101a-3p. Furthermore, reduced *Qki* expression by 23% and 12% was shown by miR-30b-5p and miR-101-3p activity, respectively. In contrast, expression of

miR-30b-5p and miR-101a-3p was increased (by 3-fold and 1.5-fold, respectively) following miRNA transfection of both miRNAs in SH-SY5Y cells. These findings can suggest the involvement of *Qki*, and hence its *Mbp* mRNA target, in dysregulated myelination processes, subsequent to downregulation of miR-30b-5p and miR-101a-3p.

[0163] In Qk^{v} (quaking viable) mice, which carry a certain mutation in *Qki*, the rate of synthesis of MBP by oligodendrocytes was shown to be unaffected, but the level of *Mbp* mRNA was reduced. This suggests that the QKI protein could regulate myelination in the CNS via alternative pathways to oligodendrocyte differentiation. Oligodendrocytes of wild-type mice express three major *Qki* mRNA isoforms, encoding *Qk*i-5, *Qki*-6 and *Qki*-7. While *Qki*-6 and *Qki*-7 are cytoplasmic, *Qki*-5 is nucleic. QKI RNA binding proteins bind a short element in the *Mbp* 3'UTR. Elevated levels of *Qki*-5 were shown to cause nuclear export defects of *Mbp* mRNA in oligodendrocytes, leading to lower levels of MBP protein levels, especially at distal branching sites.

[0164] Stressed mice that showed higher RN levels of *Qki* mRNA, showed lower RN levels of *Mbp* mRNA. This effect was reversed under citalopram treatment. Furthermore, the same effects were seen in protein levels of both QKI and MBP. Expression levels of the *Qki*-5 isoform were higher, though without statistical significance, in the RN of stressed mice than in citalopram treated mice, while *Qki*-7 isoform levels were similar for both groups. This suggests that nuclear retention of *Mbp* mRNA by *Qki*-5 might be the reason for myelin deficits in chronically stressed mice.

[0165] To verify that the observed changes were unique to the RN, we also tested mRNA and protein levels of *Qki* and *Mbp* in the superior colliculus (SC), a tissue located above the RN, but involved in a completely different circuit. Neither mRNA or protein expression levels of *Qki* or *Mbp* differed in this tissue between stressed mice and stressed mice treated with citalopram. These results imply the specific and unique impact of SSRIs on the RN in treating myelination defects through regulated expression of *Qki*.

[0166] To investigate the effect of the observed molecular changes on CNS myelin structures, TEM imaging and analysis of the RN tissue from mice of all four

groups was performed. The *g*-ratio of axons from stressed mice was significantly lower than that of control mice, or than stressed mice that were treated with citalopram. As a lower *g*-ratio represents higher myelin thickness in specific axons, the *g*-ratio indicated thicker myelin in stressed mice than in control mice, or than stressed mice treated with citalopram. However, images of the axons revealed a different picture, in which myelin sheaths of axons in stressed mice were not compressed and gaps appeared between the myelin sheaths. This effect did not present in myelin of axons from control mice or from stressed mice treated with citalopram. These gaps cause the myelinated axons to show "thicker" myelin. MBP is known as essential for compaction of adjacent membrane surfaces into dense myelin stacks. This is primarily based on the observation of loosely compacted myelin in *shiverer* mice that carry a mutation in the MBP gene. Nuclear retention of *Mbp* that leads to less MBP protein in the distal areas of oligodendrocyte branching sites seems to be the cause of the loosely compacted myelin sheaths observed in mice following the CUS protocol. Properly compacted myelin in RN axons of stressed mice treated with citalopram suggests a mechanism by which SSRIs can affect and ameliorate depression, by directly affecting oligodendrocytes and correcting myelin deficits, and not only through serotonin levels and reuptake.

[0167] The present disclosure demonstrates a role for miR-30b-5p and miR-101a-3p, and their target gene *Qki,* in the antidepressant mode of action of SSRI therapeutics, such as citalopram. Figure 7 relies on the knowledge that SSRIs block the reuptake of serotonin by pre-synaptic SERT, but that depression symptoms are not immediately alleviated, and that *Qki* is highly expressed in brain oligodendrocytes, and affects myelination processes. It is therefore suggested that chronic stress affects the RN, which causes reduced expression of miR-30-5p and miR-101a-3p, via yet unknown pathways. This in turn causes the overexpression of *Qki*, one of their gene targets, specifically isoform *Qki*-5, which induces nuclear retention of *Mbp* mRNA, and lower levels of MBP protein at distal areas of the oligodendrocytes. As the MBP protein is required for correct myelin ensheathing of axons, this leads to insufficient compacting of the myelin sheaths. These deficits in oligodendrocyte and myelin function may disturb

signal transduction from the RN along their projections to further limbic system tissues, which may, in turn, instigate depressive symptoms.

[0168] A second aspect of this disclosure suggests that SSRI treatment causes increased transcription of RN oligodendrocytes miR-30b-5p and miR-101a-3p, which in turn restores lower levels of *Qki* mRNA and protein. This results in reduced nuclear retention of *Mbp* by *Qki*-5, which enables sufficient amounts of *Mbp* mRNA to move from the oligodendrocyte's nucleus to the cytoplasm and allows normal levels of MBP protein at distal areas. Adequate amounts of MBP protein enhance myelin repair processes, specifically correcting stress-induced dense compacting of myelin sheaths. This aids in recovering correct signal transduction in the projections that ascend from the RN, and amelioration of depressive symptoms instigated by chronic stress of affected individuals.

[0169] The present disclosure demonstrates the involvement of antidepressant drugs in myelination processes of RN neuronal axons. This work showed that *Qki*, a gene expressed in oligodendrocytes that interferes with proper myelination by inhibition of extra-nuclear transport of *Mbp* mRNA to the cytosol, is regulated by both miR-30b-5p and miR-101a-3p. Indeed, under chronic stress, both these miRNAs were downregulated and *Qki* was upregulated. This resulted in impaired MBP protein levels and an adverse effect on RN neuron myelination. Consistent with this tentative mechanism of action, SSRI treatment affects oligodendrocytes and upregulates the expression of both the abovementioned miRNAs. This in turn downregulates *Qki* and restores normal levels of *Mbp* mRNA and myelin functions.

[0170] In conclusion, the disclosers detected specific gene and miRNA changes in RN of stressed mice, who were or were not treated with citalopram. Moreover, we identified changes in myelin compaction in RN of stressed mice. Therefore, the disclosers propose miR-30b-5p and miR-101a-3p, together with *Qki,* as SSRI response biomarkers in the RN of MDD models. The present disclosure expands the understanding of axon myelination deficits in MDD and other disorders and opens new venues for developing oligodendrocyte-targeted antidepressant therapeutics, including miRNA mimics.

CLAIMS

1. A method for treating a condition associated with myelin structural deficiencies in a subject, comprising:

administering to a subject a therapeutically effective amount of a selective serotonin reuptake inhibitor (SSRI);

wherein the SSRI increases expression levels of at least one of miR-30b-5p and miR-101-3p;

wherein miR-30b-5p and miR-101-3p downregulate Qki; and

wherein reduced expression of Qki causes increased expression of Myelin Basic Protein (MBP) thereby improving myelin structure in neurons.

2. The method of claim 1, wherein miR-30b-5p and miR-101-3p downregulate isoform Qki-5 of Qki.

3. The method of claim 1, wherein the SSRI is citalopram.

4. The method of claim 1, wherein expression of miR-30b-5p, miR-101-3p, and Qki are restored to normal levels.

5. A composition for treating a condition associated with myelin structural deficiencies in a subject, comprising:

a therapeutically effective amount of SSRI.

6. The composition of claim 5, wherein the SSRI is citalopram.

7. A method of detecting the presence of a condition characterized by myelin structural deficiencies in a subject, comprising:

obtaining a biological sample from the subject;

measuring expression levels of miR-30b-5p and miR-101a-3p in the biological sample;

comparing the measured expression levels to a control;

wherein decreased expression levels of miR-30b-5p and miR-101a-3p in the biological sample as compared to the control indicates the presence of the condition; and

wherein comparable expression levels of miR-30b-5p and miR-101a-3p in the biological sample as compared to the control indicates the absence of the condition.

8. The method of claim 7, wherein the condition is selected from the group consisting of Major Depressive Disorder (MDD), schizophrenia, alcoholism, bipolar disorder, Alzheimer's disease, Parkinson's disease, autism, anorexia, post-traumatic stress disorder (PTSD), addiction, multiple sclerosis, and Generalized Anxiety Disorder (GAD)

9. A method of assessing the efficacy of an SSRI treatment in a subject with a condition, the method comprising:

administering an SSRI to the subject;

obtaining a first biological sample from the subject before SSRI administration;

obtaining a second biological sample from the subject after SSRI administration;

measuring expression levels in the first biological sample and the second biological sample of at least one of miR-30b-5p, miR-101a-3p, and QKI;

comparing the expression levels in the first biological sample with expression levels in the second biological sample of at least one of miR-30b-5p, miR-101a-3p, and QKI;

wherein increased expression levels of miR-30b-5p and miR-101a-3p in the second biological sample as compared to the first biological sample indicates a therapeutic response to the SSRI treatment; and

wherein decreased expression levels of Qki in the second biological sample as compared to the first biological sample indicates a therapeutic response to the SSRI treatment.

10. The method of claim 9, further comprising:

measuring expression levels of miR-30b-5p and miR-101a-3p in the first biological sample and the second biological sample.

11. The method of claim 9, further comprising:

measuring expression levels of Qki in the first biological sample and the second biological sample.

12. The method of claim 9, wherein the SSRI is selected from the group consisting of citalopram, dapoxetine, escitalopram, fluoxetine, fluvoxamine, paroxetine, sertraline, and vortioxetine.

13. The method of claim 9, wherein Qki is isoform Qki-5.

14. A method of developing therapeutic agents for treating a condition characterized by myelin structural deficiencies in a subject, comprising:

identifying agents that modulate expression levels of at least one of miR-30b-5p, miR-101a-3p, and Qki;

testing the agents for their ability to increase expression levels of miR-30b-5p and miR-101a-3p in the subject or testing the agents for their ability to decrease expression levels of Qki in the subject; and

selecting agents that either increase expression levels of miR-30b-5p and miR-101a-3p or decrease expression levels of Qki for further development as therapeutic agents.

15. The method of claim 14, wherein the agents include miRNA mimics;

wherein the miRNA mimics downregulate Qki.

16. The method of claim 14, further wherein:

the agents comprise an Adeno-Associated Virus (AAV), the AAV comprising expression constructs encoding at least one miRNA; and

wherein the miRNA downregulates Qki.

17. A composition for treating a condition characterized by myelin structural deficiencies in a subject, comprising:

an AAV; and

the AAV comprising expression constructs encoding at least one of miR-30b-5p and miR-101-3p.

18. The composition of claim 17, wherein the AAV comprises expression constructs of both miR-30b-5p and miR-101-3p.

19. A method of treating a condition characterized by myelin structural deficiencies in a subject, comprising:

administering to the subject a therapeutically effective amount of an AAV, the AAV comprising expression constructs encoding at least one of miR-30b-5p and miR-101-3p.

20. The method of claim 19, wherein the administration is performed through stereotactic injection of the AAV into the Raphe Nuclei (RN).

21. The method of claim 20, wherein the stereotactic injection is administered at the following approximate coordinates:

anterior-posterior (AP) axis: -4.60;

dorso-ventral (DV) axis: -3 relative to the Bregma point and dura mater level.

22. A composition for treating a condition characterized by myelin structural deficiencies in a subject, comprising:

a delivery system comprising at least one of encapsulated miR-30b-5p and encapsulated miR-101-3p.

23. The composition of claim 22, wherein the delivery system is suitable for intranasal delivery.

24. A method of treating a condition characterized by myelin structural deficiencies in a subject using the composition of claim 22, comprising:

administering a therapeutically effective amount of the composition of claim 22 into the nasal cavity of the subject.

25. The method of any one of claims 1, 7, 9, 14, 19, and 24, wherein the condition is Major Depressive Disorder (MDD).

26. The method of any one of claims 1, 7, 9, 14, 19, and 24, wherein the condition is schizophrenia.

27. The method of any one of claims 1, 7, 9, 14, 19, and 24, wherein the condition is alcoholism.

28. The method of any one of claims 1, 7, 9, 14, 19, and 24, wherein the condition is bipolar disorder.

29. The method of any one of claims 1, 7, 9, 14, 19, and 24, wherein the condition is Alzheimer's disease.

30. The method of any one of claims 1, 7, 9, 14, 19, and 24, wherein the condition is Parkinson's disease.

31. The method of any one of claims 1, 7, 9, 14, 19, and 24, wherein the condition is autism.

32. The method of any one of claims 1, 7, 9, 14, 19, and 24, wherein the condition is anorexia.

33. The method of any one of claims 1, 7, 9, 14, 19, and 24, wherein the condition is post-traumatic stress disorder (PTSD).

34. The method of any one of claims 1, 7, 9, 14, 19, and 24, wherein the condition is addiction.

35. The method of any one of claims 1, 7, 9, 14, 19, and 24, wherein the condition is multiple sclerosis.

36. The method of any one of claims 1, 7, 9, 14, 19, and 24, wherein the condition is Generalized Anxiety Disorder (GAD).

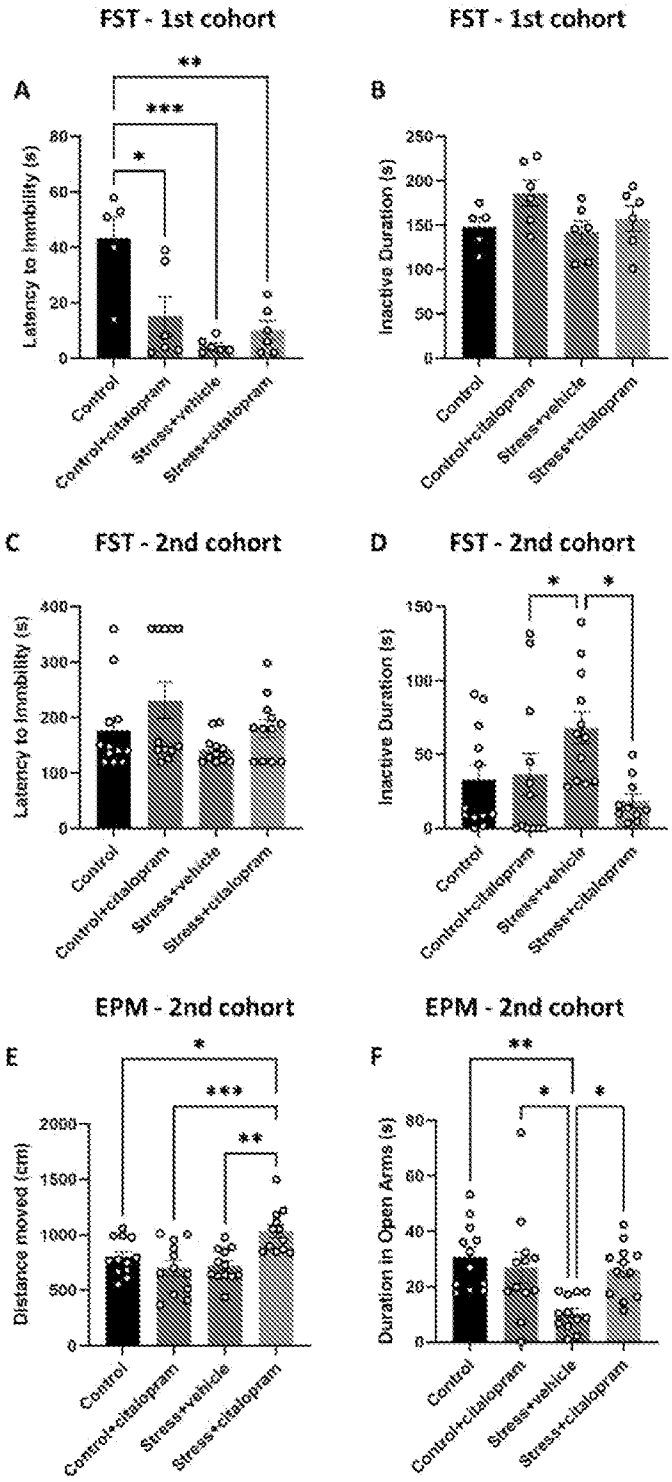
A
FST - 1st cohort
Latency to immbility (s)
Control
Control+citalopram
Stress+vehicle
Stress+citalopram
B
FST - 1st cohort
Inactive Duration (s)
C
FST - 2nd cohort
D
FST - 2nd cohort
E
EPM - 2nd cohort
Distance moved (cm)
F
EPM - 2nd cohort
Duration in Open Arms (s)

FIG 1

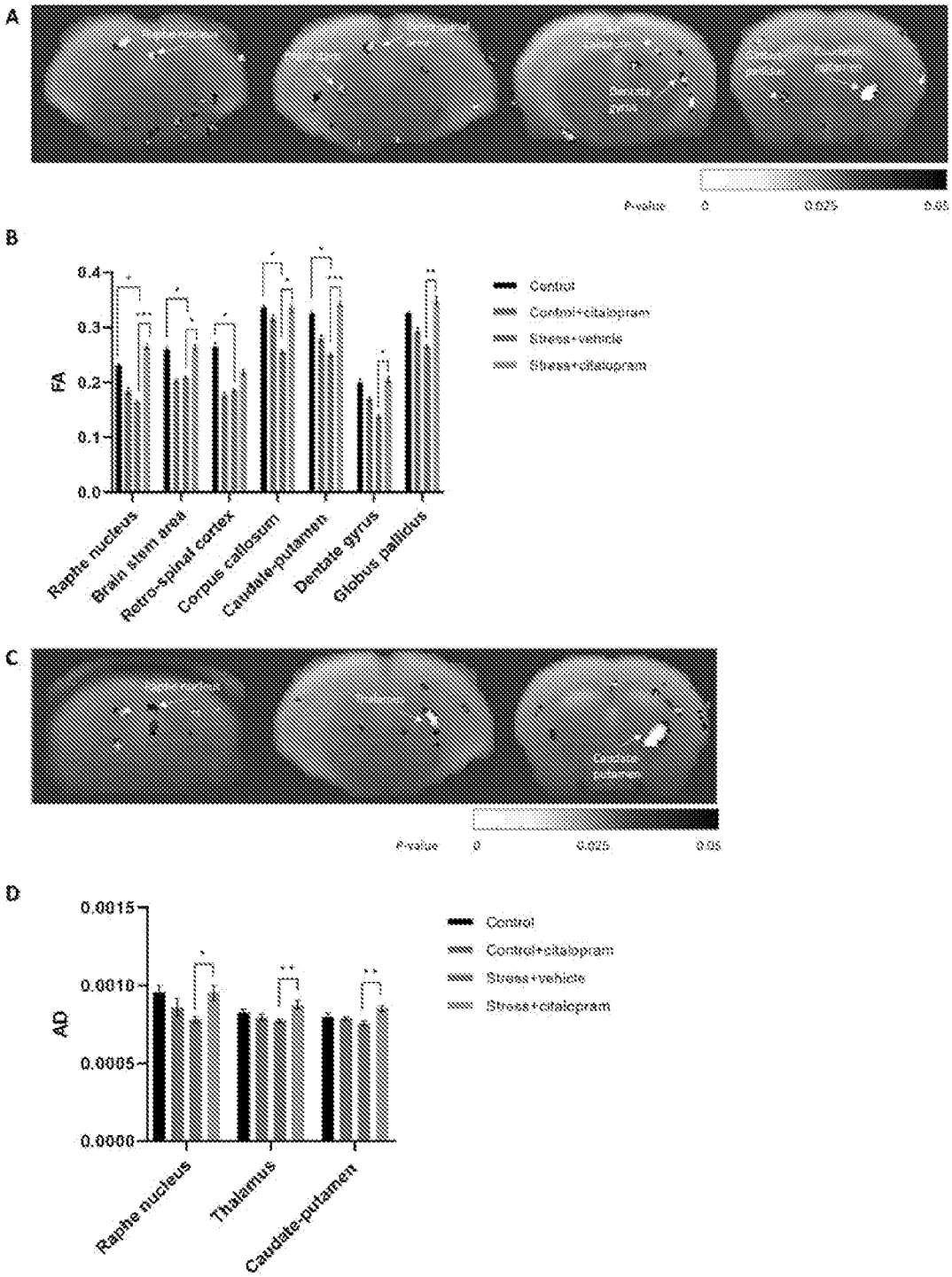
A
P-value
0
0.025
0.05
B
FA
0.4
0.3
0.2
0.1
0.0
Control
Control+citalopram
Stress+vehicle
Stress+citalopram
Raphe nucleus
Brain stem area
Retro-spinal cortex
Corpus callosum
Caudate-putamen
Dentate gyrus
Globus pallidus
C
P-value
0
0.025
0.05
D
AD
0.0015
0.0010
0.0005
0.0000
Control
Control+citalopram
Stress+vehicle
Stress+citalopram
Raphe nucleus
Thalamus
Caudate-putamen

FIG 2

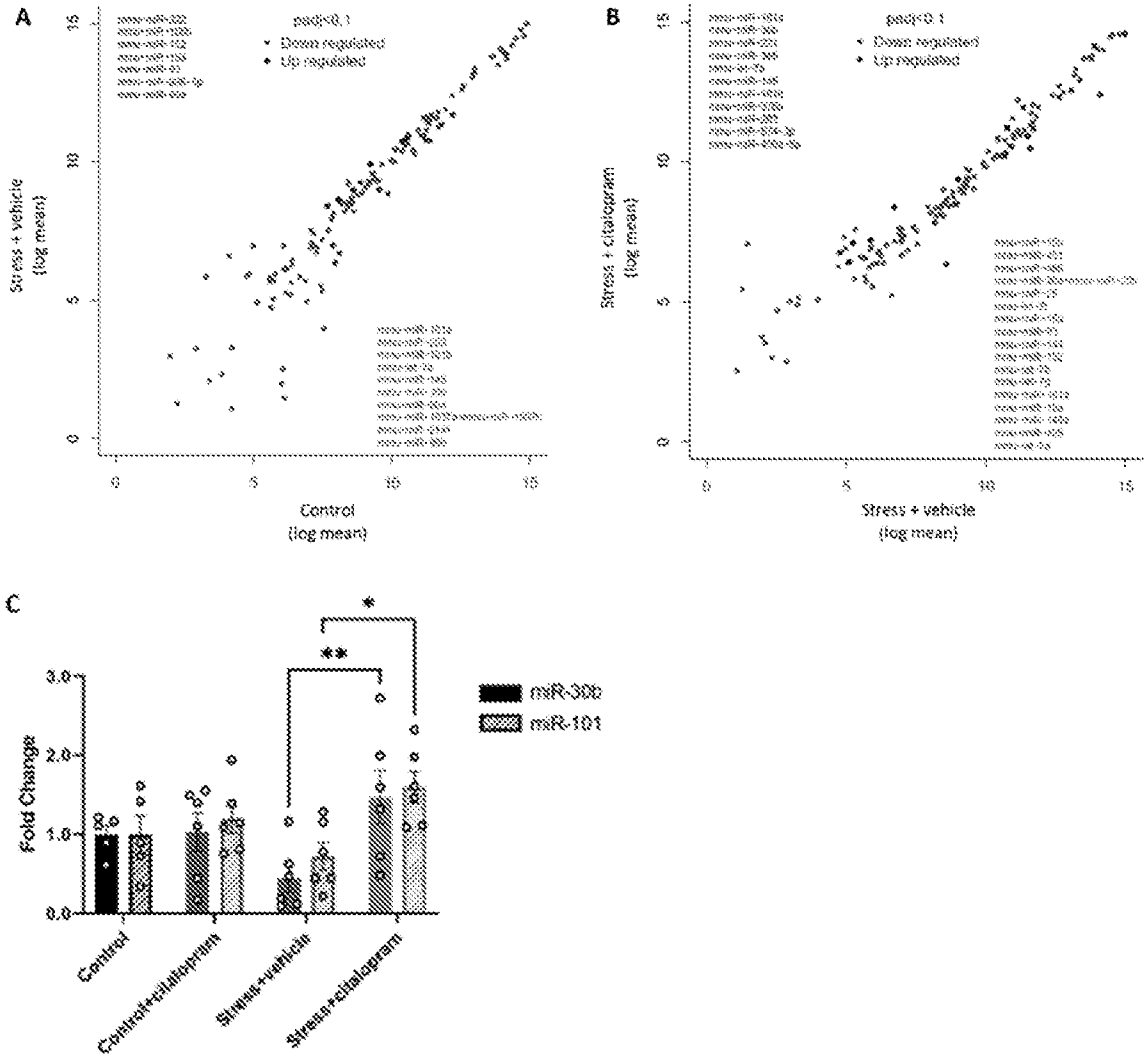
A
padj<0.1
Down regulated
Up regulated
Stress + vehicle (log mean)
Control (log mean)
B
padj<0.1
Down regulated
Up regulated
Stress + citalopram (log mean)
Stress + vehicle (log mean)
C
miR-30b
miR-101
Fold Change
Control
Control+citalopram
Stress+vehicle
Stress+citalopram

FIG 3

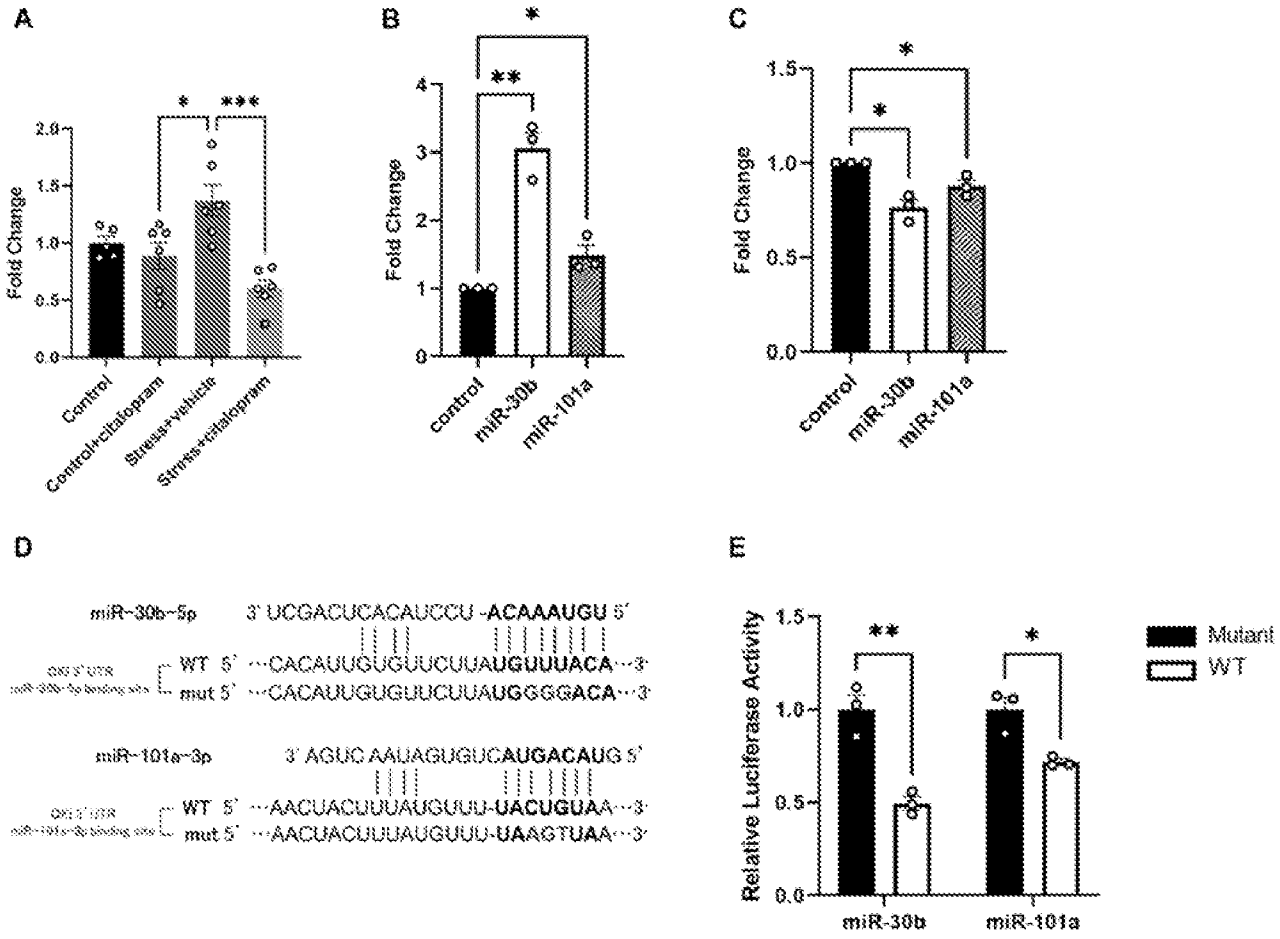
A
Fold Change
Control
Control+citalopram
Stress+vehicle
Stress+citalopram
B
Fold Change
control
miR-30b
miR-101a
C
Fold Change
control
miR-30b
miR-101a
D
miR-30b-5p 3' UCGACUCACAUCCU-ACAAAUGU 5'
WT 5' ···CACAUUGUGUUCUUAUGUUUACA···3'
mut 5' ···CACAUUGUGUUCUUAUGGGGACA···3'
miR-101a-3p 3' AGUC AAUAGUGUCAUGACAUG 5'
WT 5' ···AACUACUUUAUGUUU-UACUGUAA···3'
mut 5' ···AACUACUUUAUGUUU-UAAGTUAA···3'
E
Relative Luciferase Activity
miR-30b
miR-101a
Mutant
WT

FIG 4

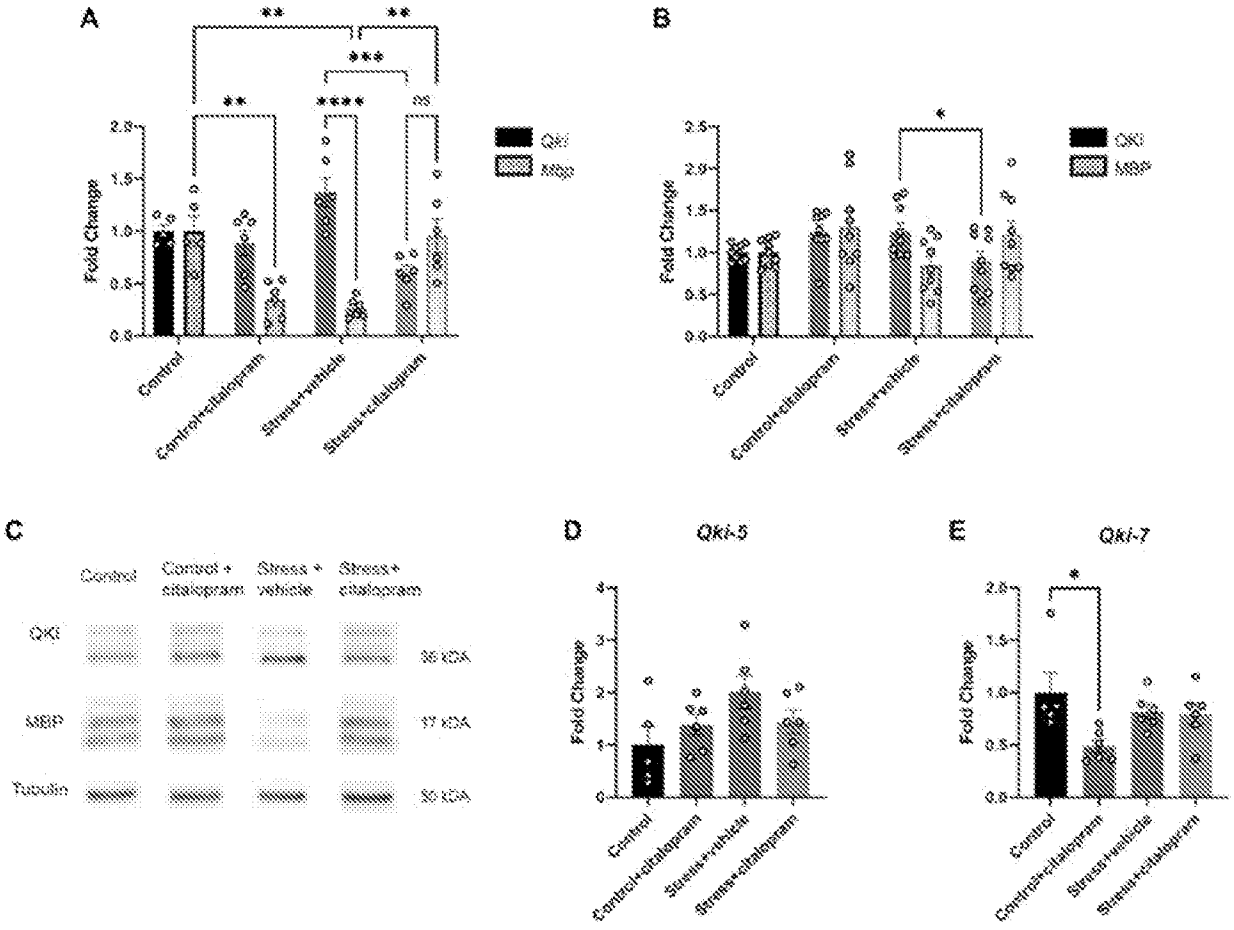
A
B
C
D
E
Fold Change
Control
Control+citalopram
Stress+vehicle
Stress+citalopram
QKI
MBP
Tubulin
Qki-5
Qki-7
ns

FIG 5

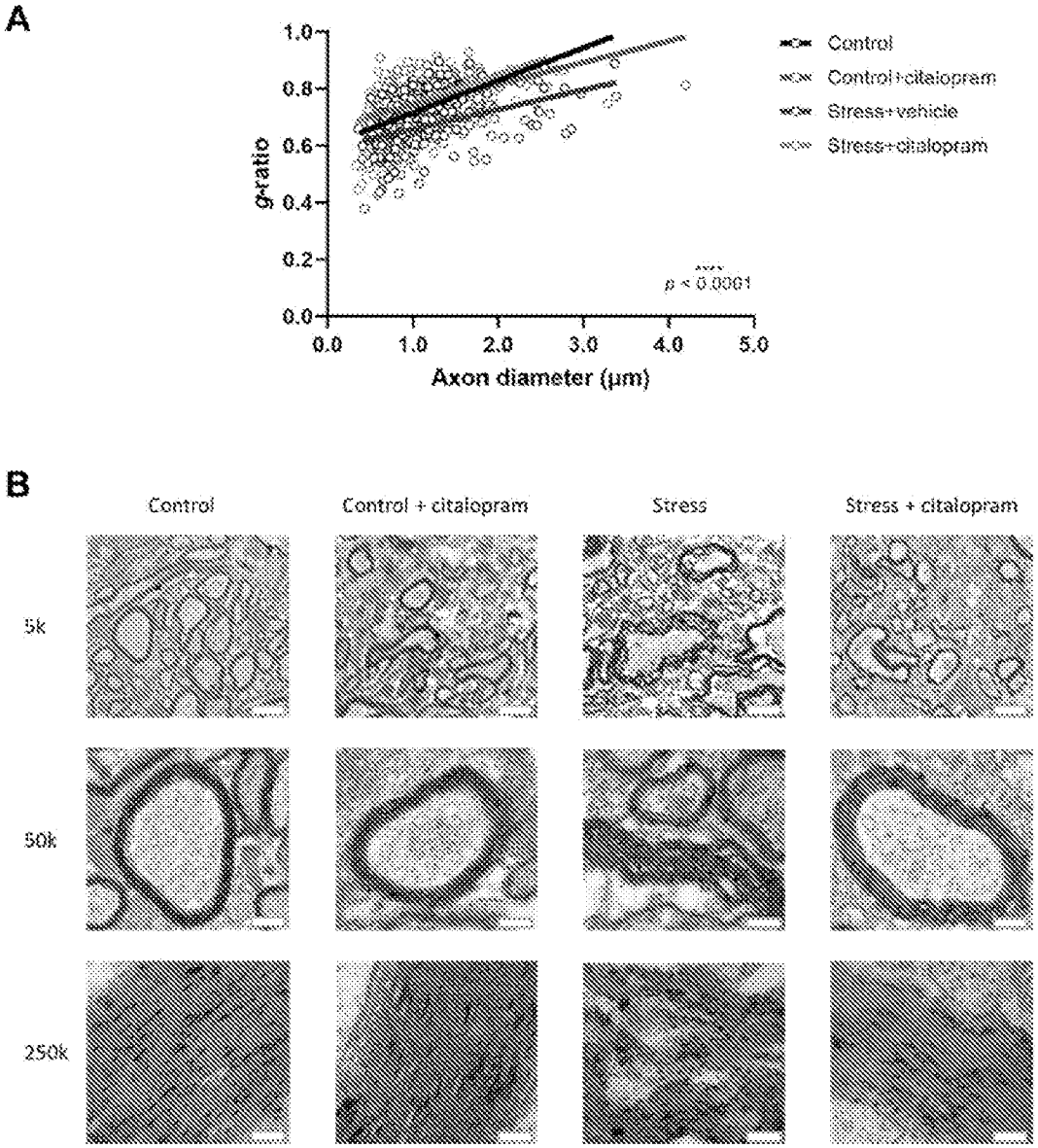
A
g-ratio
Axon diameter (µm)
Control
Control+citalopram
Stress+vehicle
Stress+citalopram
p < 0.0001
B
Control
Control + citalopram
Stress
Stress + citalopram
5k
50k
250k

FIG 6

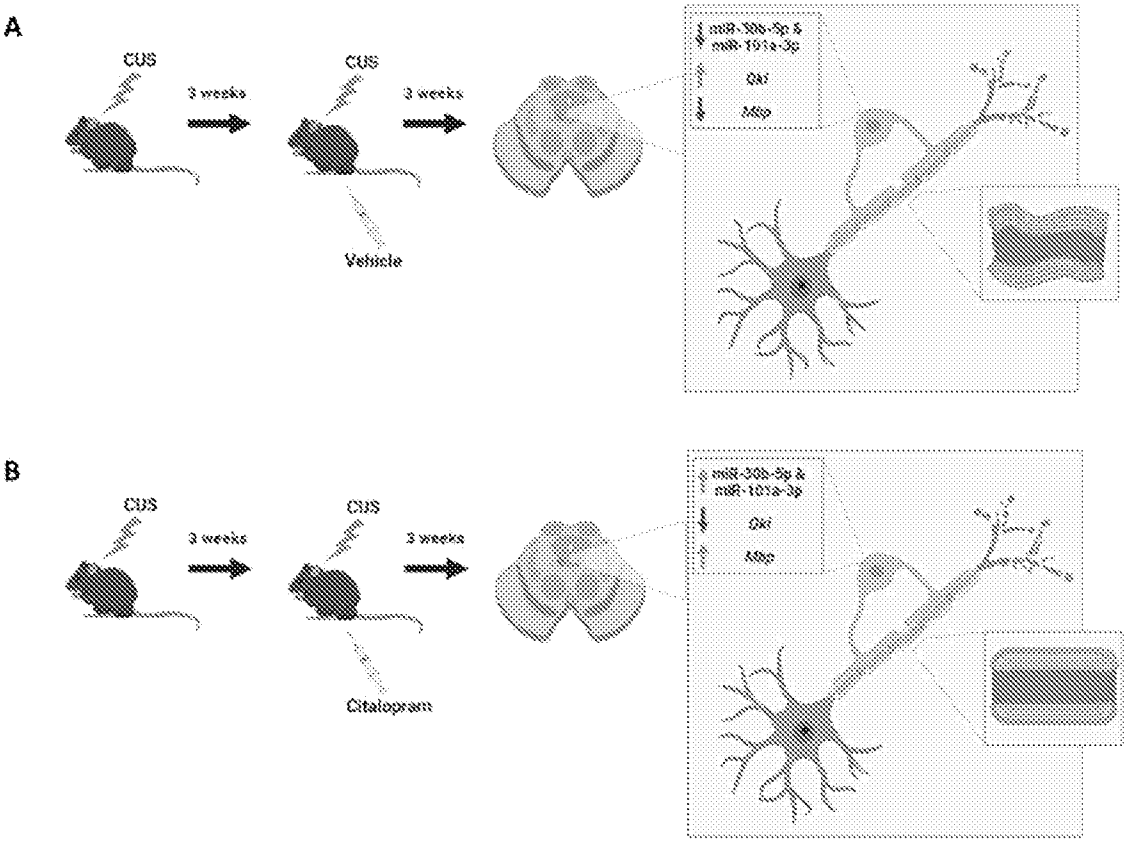
A
CUS
3 weeks
CUS
3 weeks
Vehicle
B
CUS
3 weeks
CUS
3 weeks
Citalopram

FIG 7

INTERNATIONAL SEARCH REPORT

International application No.
PCT/IB2024/057742

A. CLASSIFICATION OF SUBJECT MATTER

A61K 31/04(2024.01)i; ***C12Q 1/68***(2024.01)i; ***A61P 25/18***(2024.01)i; ***A61P 25/00***(2024.01)i; ***A61P 25/28***(2024.01)i; ***C12Q 1/686***(2024.01)i
CPC:A61K 31/04; C12Q 1/68; A61P 25/18; A61P 25/00; A61P 25/28; C12Q 1/686

According to International Patent Classification (IPC) or to both national classification and IPC

B. FIELDS SEARCHED

Minimum documentation searched (classification system followed by classification symbols)

A61K 31/04; C12Q 1/68; C12N 15/113; A61P 25/00; A61P 25/28; A61P 25/18; C12Q 1/686
CPC:A61K 31/04; C12Q 1/68; C12N 15/113; A61P 25/00; A61P 25/28; A61P 25/18; C12Q 1/686

Documentation searched other than minimum documentation to the extent that such documents are included in the fields searched

Electronic data base consulted during the international search (name of data base and, where practicable, search terms used)

Databases consulted: Eponline, Esp@cenet, Google Patents, PubMed, Google Scholar, PatBase Search terms used: SSRI, myelin, MicroRNA

C. DOCUMENTS CONSIDERED TO BE RELEVANT

Category*	Citation of document, with indication, where appropriate, of the relevant passages	Relevant to claim No.
	Seiger, R., et al. "The influence of acute SSRI administration on white matter microstruct ure in patients suffering from major depressive disorder and healthy controls." International Journal of Neuropsychopharmacology 24.7 (2021): 542-550. https://academic.oup.com/ijnp/article/24/7/542/6154678?login=true Retrieved on: 28/10/2024 (2021/03/01)	
X	abstract, 2nd paragraph on 1st column on p. 548, figure 1	1-6
Y		9-13
	Chen, Siyi, Laura Bennet, and Ailsa L. McGregor. "Delayed citalopram administration reduces brain inflammation and enhances skilled motor function after ischaemic stroke in 'MacGreen' mice." European Journal of Neuroscience 55.5 (2022): 1344-1355. https://onlinelibrary.wiley.com/doi/full/10.1111/ejn.15601 Retrieved on: 29/10/2024 (2022/01/20)	
X	abstract, figure 5	1-6
Y		9-13

☑ Further documents are listed in the continuation of Box C. ☐ See patent family annex.

* Special categories of cited documents:
"A" document defining the general state of the art which is not considered to be of particular relevance
"D" document cited by the applicant in the international application
"E" earlier application or patent but published on or after the international filing date
"L" document which may throw doubts on priority claim(s) or which is cited to establish the publication date of another citation or other special reason (as specified)
"O" document referring to an oral disclosure, use, exhibition or other means
"P" document published prior to the international filing date but later than the priority date claimed
"T" later document published after the international filing date or priority date and not in conflict with the application but cited to understand the principle or theory underlying the invention
"X" document of particular relevance; the claimed invention cannot be considered novel or cannot be considered to involve an inventive step when the document is taken alone
"Y" document of particular relevance; the claimed invention cannot be considered to involve an inventive step when the document is combined with one or more other such documents, such combination being obvious to a person skilled in the art
"&" document member of the same patent family

Date of the actual completion of the international search	Date of mailing of the international search report
04 November 2024	**06 November 2024**

Name and mailing address of the ISA/IL	Authorized officer
Israel Patent Office **Technology Park, Bldg.5, Malcha, Jerusalem, 9695101, Israel** **Israel** Telephone No. **972-73-3927176** Email: **pctoffice@justice.gov.il**	**PERLMAN Noa** Telephone No.

C. DOCUMENTS CONSIDERED TO BE RELEVANT

Category*	Citation of document, with indication, where appropriate, of the relevant passages	Relevant to claim No.
	Kroeze, Y., et al. "Long-term consequences of chronic fluoxetine exposure on the expressio n of myelination-related genes in the rat hippocampus." Translational psychiatry 5.9 (2015): e642-e642. https://www.nature.com/articles/tp2015145 Retrieved on: 29/10/2024 (2015/09/22)	
X	abstract, 1st paragraph on 2nd column on p. 2	1-6
Y		9-13
	Liu, S., et al. "The early growth response protein 1-miR-30a-5p-neurogenic differentiation factor 1 axis as a novel biomarker for schizophrenia diagnosis and treatment monitoring." Translational Psychiatry 7.1 (2017): e998-e998. https://www.nature.com/articles/tp2016268 Retrieved on: 30/10/2024 (2017/01/10)	
X	1st paragraph on 1st column on p. 6, 2nd column on p. 1	7,8
Y		9-36
	Maciak, Karina, Angela Dziedzic, and Joanna Saluk. "Remyelination in multiple sclerosis from the miRNA perspective." Frontiers in Molecular Neuroscience 16 (2023): 1199313. https://www.frontiersin.org/journals/molecular-neuroscience/articles/10.3389/fnmo l.2023.1199313/full Retrieved on: 30/10/2024 (2023/06/01)	
Y	abstract, 3rd paragraph on 2nd column on p. 02, 4th paragraph on 2nd column on p. 03, 4th paragraph on 2nd column on p. 03, 1st paragraph on 1st column on p. 06	14-18
	Higuchi, Fumihiro, et al. "Hippocampal microRNA-124 enhances chronic stress resilience in mice." Journal of Neuroscience 36.27 (2016): 7253-7267. https://www.jneurosci.org/content/36/27/7253.short Retrieved on: 31/10/2024 (2016/07/06)	
Y	1st paragraph on 1st column on p. 7256, 2nd paragraph on 1st column on p 7254, 3rd paragraph on 2nd column on p. 7262	9-13,19-36